NLR network mediates immunity to diverse plant pathogens

Chih-Hang Wu[a], Ahmed Abd-El-Haliem[b], Tolga O. Bozkurt[a,c], Khaoula Belhaj[a], Ryohei Terauchi[d,e], Jack H. Vossen[b], and Sophien Kamoun[a,1]

[a]The Sainsbury Laboratory, Norwich Research Park, Norwich NR4 7UH, United Kingdom; [b]Plant Breeding, Wageningen University and Research, Wageningen 6708 PB, The Netherlands; [c]Department of Life Sciences, Imperial College London, London SW7 2AZ, United Kingdom; [d]Division of Genomics and Breeding, Iwate Biotechnology Research Center, Iwate 024-0003, Japan; and [e]Laboratory of Crop Evolution, Graduate School of Agriculture, Kyoto University, Kyoto 606-8501, Japan

Edited by Jeff L. Dangl, University of North Carolina at Chapel Hill, Chapel Hill, NC, and approved June 19, 2017 (received for review February 13, 2017)

Both plants and animals rely on nucleotide-binding domain and leucine-rich repeat-containing (NLR) proteins to respond to invading pathogens and activate immune responses. An emerging concept of NLR function is that "sensor" NLR proteins are paired with "helper" NLRs to mediate immune signaling. However, our fundamental knowledge of sensor/helper NLRs in plants remains limited. In this study, we discovered a complex NLR immune network in which helper NLRs in the NRC (NLR required for cell death) family are functionally redundant but display distinct specificities toward different sensor NLRs that confer immunity to oomycetes, bacteria, viruses, nematodes, and insects. The helper NLR NRC4 is required for the function of several sensor NLRs, including Rpi-blb2, Mi-1.2, and R1, whereas NRC2 and NRC3 are required for the function of the sensor NLR Prf. Interestingly, NRC2, NRC3, and NRC4 redundantly contribute to the immunity mediated by other sensor NLRs, including Rx, Bs2, R8, and Sw5. NRC family and NRC-dependent NLRs are phylogenetically related and cluster into a well-supported superclade. Using extensive phylogenetic analysis, we discovered that the NRC superclade probably emerged over 100 Mya from an NLR pair that diversified to constitute up to one-half of the NLRs of asterids. These findings reveal a complex genetic network of NLRs and point to a link between evolutionary history and the mechanism of immune signaling. We propose that this NLR network increases the robustness of immune signaling to counteract rapidly evolving plant pathogens.

immunity | host–microbe interactions | evolution

Plants and animals rely on nucleotide-binding domain and leucine-rich repeat-containing (NLR) proteins to activate immune responses to invading pathogens (1–3). NLRs are among the most diverse and rapidly evolving protein families in plants (4, 5). They are modular proteins that broadly fall into two classes based on their N-terminal domain, which is either a Toll-interleukin 1 receptor or a coiled coil (CC) domain (6). Most plant disease resistance genes encode NLR receptors that detect effector proteins secreted by pathogens by either directly binding them or indirectly binding them via effector-targeted host proteins (3, 7). An emerging model is that "sensor" NLRs dedicated to detecting pathogen effectors require "helper" NLRs to initiate immune signaling, resulting in a hypersensitive cell death response that restricts pathogen invasion (8–11). Although paired NLRs have been described across flowering plants, the degree to which plant NLRs have evolved to form higher order networks is poorly known.

Solanaceae form one of the most species-rich plant families that include major agricultural crops, such as potato, tomato, and pepper (12). The extensive breeding efforts for improving disease resistance within this family have led to the identification of many NLR-type disease resistance genes from wild relatives (13, 14). To date, over 20 NLR-type disease resistance genes have been identified from different solanaceous species, which confer resistance to infection by diverse and destructive pathogens and pests, including the oomycete *Phytophthora infestans*, tomato spotted wilt virus (TSWV), and potato cyst and root-knot nematodes (13, 14). Several of these solanaceous NLR-type disease resistance genes have been deployed in agriculture through traditional breeding, cisgenesis, or transgenesis (14, 15). For example, *Rpi-blb2* has been introgressed into potato cultivars to confer broad-spectrum resistance to isolates of *P. infestans* (16). *Mi-1.2*, an ortholog of *Rpi-blb2*, confers resistance to root-knot nematodes, aphids, and whiteflies in cultivars of tomato (17–19). Expression of the pepper gene *Bs2* in tomato confers resistance to the bacterial spot pathogen *Xanthomonas campestris* pv. *vesicatoria* (20). *Sw5b*, a gene from the wild tomato species *Solanum peruvianum*, mediates resistance against TSWV in tomato (21). Furthermore, introgression of *Rx* and *Gpa2* into potato confers resistance to potato virus X (PVX) and potato cyst nematode, respectively (22, 23).

In addition to their agricultural importance, the Solanaceae and their NLRs are a great experimental model system for understanding plant immunity. Many of the cloned solanaceous NLR genes recapitulate their effector recognition and disease resistance phenotypes when expressed into the model plant *Nicotiana benthamiana*. Classic examples of mechanistic studies of solanaceous NLRs in *N. benthamiana* include the Prf/Pto complex which mediates resistance to *Pseudomonas syringae* through association with the effectors AvrPto and AvrPtoB (24–26), and the Rx/RanGAP2 complex, which confers resistance to PVX by recognizing the coat protein (23, 27–29). These studies contributed to our understanding of NLR function, particularly the role of effector-associated proteins in activating immunity.

Genome-wide annotation and cross-species comparison revealed that NLR genes are often dramatically expanded in the genomes of flowering plants, reaching hundreds of genes in diverse species like rice, soybean, grapevine, and potato (30). Across different plant species, NLR genes belonging to different phylogenetic clades may show distinct expansion and gene loss

Significance

Plant and animal nucleotide-binding domain and leucine-rich repeat-containing (NLR) proteins often function in pairs to mediate innate immunity to pathogens. However, the degree to which NLR proteins form signaling networks beyond genetically linked pairs is poorly understood. In this study, we discovered that a large NLR immune signaling network with a complex genetic architecture confers immunity to oomycetes, bacteria, viruses, nematodes, and insects. The network emerged over 100 Mya from a linked NLR pair that diversified into up to one-half of the NLRs of asterid plants. We propose that this NLR network increases robustness of immune signaling to counteract rapidly evolving plant pathogens.

Author contributions: C.-H.W., A.A.-E.-H., T.O.B., K.B., R.T., J.H.V., and S.K. designed research; C.-H.W., A.A.-E.-H., and J.H.V. performed research; A.A.-E.-H. and J.H.V. contributed new reagents/analytic tools; C.-H.W. and S.K. analyzed data; and C.-H.W. and S.K. wrote the paper.

The authors declare no conflict of interest.

This article is a PNAS Direct Submission.

[1]To whom correspondence should be addressed. Email: sophien.kamoun@tsl.ac.uk.

This article contains supporting information online at www.pnas.org/lookup/suppl/doi:10.1073/pnas.1702041114/-/DCSupplemental.

patterns, indicating that NLR evolution exhibits dynamic patterns of birth and death (4, 6, 30–32). Strong selection caused by pathogens is thought to drive functional diversification of NLR genes, which tend to be clustered in dynamic regions of plant genomes (32–34). However, despite the extensive knowledge generated through comparative genomics, the degree to which phylogeny correlates with mechanisms of NLR activation and signaling remains unclear.

In a previous study, we reported that the helper NLR proteins NLR required for cell death 2 (NRC2) and NRC3 are functionally redundant and are required for the function of the Prf/Pto complex in *N. benthamiana* (11). However, whether NRC2, NRC3, and other NRC-like genes function with other sensor NLRs remained unknown. Here, we describe another helper NLR, termed NRC4, which belongs to the NRC family. NRC4 is required for immunity triggered by Rpi-blb2, an NLR that provides resistance to *P. infestans* but is not required for Prf-mediated immunity. Surprisingly, NRC2, NRC3, and NRC4 turned out to be functionally redundant and essential for the activity of at least seven other NLRs that confer immunity to oomycetes, bacteria, viruses, nematodes, and insects. Remarkably, the NRC family and NRC-dependent NLRs fall into a well-supported phylogenetic superclade. Using extensive phylogenetic analyses of plant NLR sequences, we revealed that the NRC superclade probably evolved from a common ancestral NLR pair over 100 Mya. We conclude that NRCs and their mates form a complex genetic network that confers resistance to diverse pathogens and pests. We propose that this complex NLR network increased the evolvability and robustness of immune signaling to counteract rapidly evolving plant pathogens.

Results and Discussion

***NRC4* Is Required for Rpi-blb2–Mediated Immunity.** As part of a study performed in *N. benthamiana* to identify genetic components required for resistance to *P. infestans* conferred by the potato NLR-type gene *Rpi-blb2* (35, 36), we discovered that another NLR protein, NRC4, is required for Rpi-blb2 function (Fig. 1). Silencing of *NRC4* compromised Rpi-blb2 resistance to *P. infestans* (Fig. 1*A*) and hypersensitive cell death to the *P. infestans* effector AVRblb2 (36) (Fig. 1*B*). This phenotype was rescued by a silencing-resilient synthetic *NRC4* gene (Fig. 1 *C* and *D* and *SI Appendix*, Fig. S1 *A* and *B*), confirming that the observed phenotype was indeed caused by *NRC4* silencing. Silencing of *NRC4* did not affect Rpi-blb2 protein accumulation (*SI Appendix*, Fig. S1*C*).

Previous studies of NLR pairs reported contrasting findings on the role of the ATP-binding p-loop motif in immune signaling. In some cases, only one NLR in the complex requires the p-loop motif (37, 38), whereas the ADR1 helper NLR from *Arabidopsis thaliana* displays p-loop–independent immune activity (8). We tested the role of the p-loop in Rpi-blb2 and NRC4 functions. Mutations in either Rpi-blb2 or NRC4 p-loops abolished the hypersensitive cell death response (*SI Appendix*, Fig. S2). Thus, the classic sensor/helper NLR model is not sufficient to explain how the Rpi-blb2/NRC4 mediates immunity.

NRC4 defines a distinct clade within the NRC family (*SI Appendix*, Fig. S3*A*). Of the nine *NRC* genes in *N. benthamiana*, four were expressed to significant levels in leaves, but only *NRC4* transcript levels were reduced in *NRC4*-silenced plants (*SI Appendix*, Figs. S1*D* and S3*B*). Among the expressed genes, *NRC2* and *NRC3* are required for bacterial resistance mediated by the NLR protein Prf in *N. benthamiana* (11, 24) but were not essential for Rpi-blb2 functions in our silencing experiments (Fig. 1 *A* and *B*). In contrast, *NRC4* was not essential for Prf-mediated cell death and resistance to the bacterial pathogen *P. syringae* (Fig. 1*B* and *SI Appendix*, Fig. S4).

NRC Clade and Its Sister Clades Form a Signaling Network. Phylogenetic analyses of the complete repertoire of CNL (NLR with an N-terminal CC domain) proteins from the solanaceous plants tomato, potato, and pepper and *N. benthamiana* revealed that the NRC family groups with the Rpi-blb2 and Prf clades in a well-supported superclade (*SI Appendix*, Fig. S5). Interestingly, this superclade includes additional well-known NLRs, such as Rx (23, 27), Bs2 (20), R8 (39), Sw5b (21), R1 (40), and Mi-1.2 (17), which confer resistance to diverse plant pathogens and pests (*SI Appendix*, Fig. S5 and Table S1). This finding prompted us to test the extent to which NRC proteins are involved in immune responses mediated by these phylogenetically related disease resistance proteins.

Silencing of *NRC2* and *NRC3* affected Prf and moderately reduced the hypersensitive cell death triggered by the potato late blight resistance gene R8, but did not alter the response mediated by 12 other NLR proteins (Fig. 2). In contrast, silencing of *NRC4* compromised the hypersensitive cell death mediated by Mi-1.2, an Rpi-blb2 ortholog that provides resistance to nematodes and insects; CNL-11990^{D474V}, an autoactive mutant of a CNL of unknown function; and R1, an NLR that confers resistance to *P. infestans* (Fig. 2 and *SI Appendix*, Fig. S6*A*). Furthermore, *NRC4* silencing abolished R1-mediated disease resistance to *P. infestans*, and the phenotype was rescued by a silencing-resilient synthetic *NRC4* gene (*SI Appendix*, Fig. S6 *B–D*).

Given that the three expressed NRC proteins share extensive sequence similarity (*SI Appendix*, Fig. S7), we hypothesized that NRC2, NRC3, and NRC4 are functionally redundant for

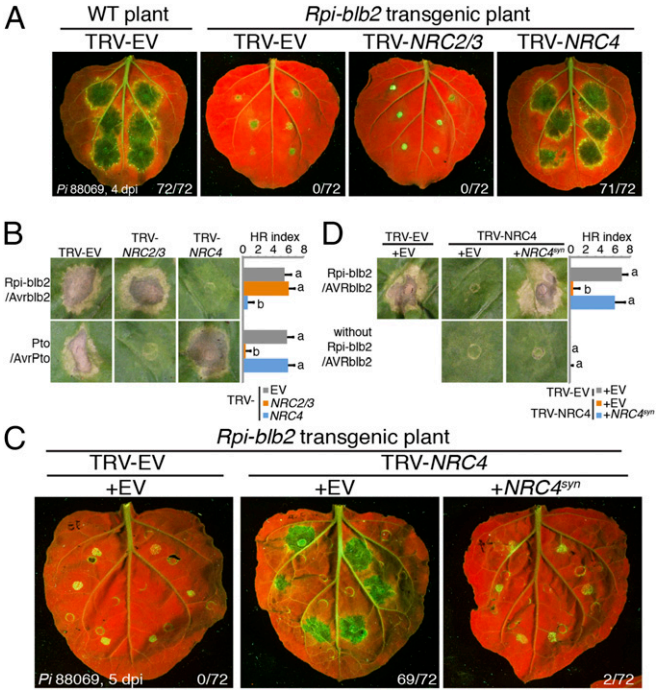

Fig. 1. *NRC4* is required for Rpi-blb2–mediated immunity. (*A*) Silencing of *NRC4* compromises Rpi-blb2–mediated resistance. *P. infestans* strain 88069 (*Pi* 88069) was inoculated on *Rpi-blb2* transgenic *N. benthamiana* preinfected with tobacco rattle virus (TRV) to silence *NRC2/3* or *NRC4*. Wild-type (WT) plant with TRV empty vector (TRV-EV) was used as a susceptible control. Experiments were repeated three times with 24 inoculation sites each time. The numbers on the right bottom of the photographs indicate the sum of spreading lesions/total inoculation sites from the three replicates. Images were taken under UV light at 4 d postinoculation (dpi). (*B*) Silencing of *NRC4* compromises Rpi-blb2– but not Prf-mediated hypersensitive cell death. Rpi-blb2/AVRblb2 or Pto/AvrPto (cell death mediated by Prf) was coexpressed in *NRC2/3*- or *NRC4*-silenced plants by agroinfiltration. HR, hypersensitive response. (*C*) Expression of silencing-resilient synthetic *NRC4* (*NRC4^{syn}*) rescues Rpi-blb2–mediated resistance in *NRC4*-silenced plants. Experiments were repeated three times with 24 inoculation sites each time. The numbers on the right bottom of the photographs indicate the sum of spreading lesion/total inoculation sites from the three replicates. Images were taken under UV light at 5 dpi. (*D*) Expression of silencing-resilient *NRC4^{syn}* rescues Rpi-blb2–mediated cell death in *NRC4*-silenced plants. HRs in *B* and *D* were scored at 7 d after agroinfiltration. Bars represent mean + SD of 24 infiltration sites. Statistical differences among the samples were analyzed with ANOVA and Tukey's honest significance difference (HSD) test ($P < 0.001$).

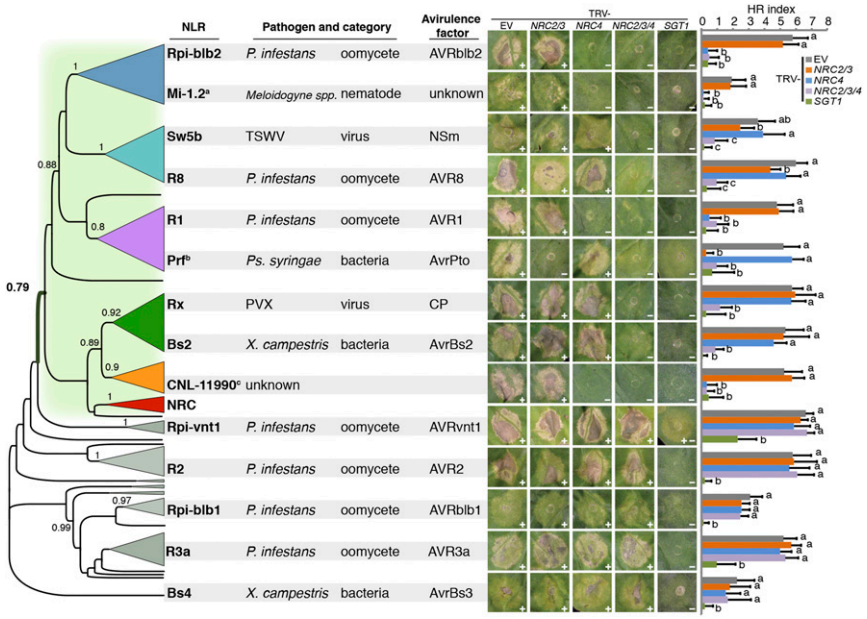

Fig. 2. NRC clade and its sister clades form a complex signaling network. (*Left*) Phylogenetic tree of CNL proteins identified from genomes of solanaceous plants, simplified from *SI Appendix*, Fig. S5. (*Center*) List of pathogens and AVR effectors sensed by the corresponding NLR immune receptors. *Ps.*, *Pseudomonas*; *X.*, *Xanthomonas*. (*Right*) Different NLR and AVR effector combinations were expressed in control (EV) and *NRC2/3-*, *NRC4-*, *NRC2/3/4-*, and *SGT1*-silenced plants by agroinfiltration. The plus symbol (+) indicates that the cell death phenotype was observed, and the minus symbol (–) indicates that the cell death phenotype was compromised. Bars represent mean + SD of 24 infiltration sites. Statistical differences among the samples were analyzed with ANOVA and Tukey's HSD test ($P < 0.001$). [a]The autoactive mutant Mi-1.2^{T557S} was used here. [b]Coexpression of Pto and AvrPto was used for testing Prf-mediated cell death. [c]The autoactive mutant CNL-11990^{D474V} was used here. Silencing of *SGT1* was used as a control that compromises cell death mediated by all of the NLRs tested here.

additional NLRs in the "NRC superclade" (Fig. 2). To test our hypothesis, we simultaneously silenced the three *NRC* genes and discovered that triple silencing of *NRC2/3/4* compromised the hypersensitive cell death mediated by Sw5b, R8, Rx, and Bs2 in addition to the five NLRs mentioned above (Fig. 2 and *SI Appendix*, Figs. S8 and S9). In contrast, triple silencing of *NRC* did not affect the hypersensitive cell death mediated by the five tested NLRs that map outside the NRC superclade (Fig. 2) and did not abolish resistance to *P. infestans* conferred by two of these NLR proteins (*SI Appendix*, Fig. S10).

We validated NRC2, NRC3, and NRC4 redundancy by complementation in the triple silencing background with silencing-resilient synthetic *NRC* (*SI Appendix*, Fig. S11). These results confirmed that the three NRC proteins display specificity to Rpi-blb2 and Prf but have redundant functions in Rx-, Bs2-, R8-, and Sw5b-mediated hypersensitive cell death (*SI Appendix*, Fig. S11).

The p-Loop Is Essential for the Activity of NRC4 in All of the Tested Combinations. We further tested whether the p-loop is essential for the activity of NRC homologs in different helper-sensor NLR combinations. The lysine (K) to arginine (R) mutation in the p-loops of NRC2 and NRC3 dramatically compromised steady-state protein accumulation (*SI Appendix*, Fig. S12*A*), prompting us to focus on NRC4 in subsequent experiments. The p-loop mutants of NRC4 failed to rescue cell death mediated by any of the sensor NLRs we tested (*SI Appendix*, Fig. S12 *B* and *C*), indicating that the p-loop is essential for NRC4-mediated immunity. These results challenge our understanding of helper NLR activation, in which proteins such as ADR1-L2 display p-loop–independent activity in NLR-triggered immunity (8). Phylogenetically, the ADR1/NRG1 family belongs to the RPW8 clade that is distantly related to the NRC family (CNL-14) (41, 42). This observation indicates that ADR1/NRG1 and the NRC families have independently evolved as helper NLRs, and may have acquired different mechanisms to activate immune signaling. Interestingly, activation of DM1/DM2d, an NLR complex that contributes to hybrid necrosis, was recently reported to require the p-loops of both NLRs (43), suggesting that not all genetic or physical NLR complexes are regulated through the same mechanism.

NRC2, NRC3, and NRC4 Redundantly Contribute to Rx-Mediated Resistance to PVX. To validate further that NRC2, NRC3, and NRC4 redundantly contribute to immunity, we examined the resistance mediated by Rx to PVX (23, 27) in plants silenced for single, double, or triple combinations of *NRC* genes. Rx-mediated resistance to PVX was only abolished in the triple silencing background, resulting in systemic spread of necrotic lesions (Fig. 3 and

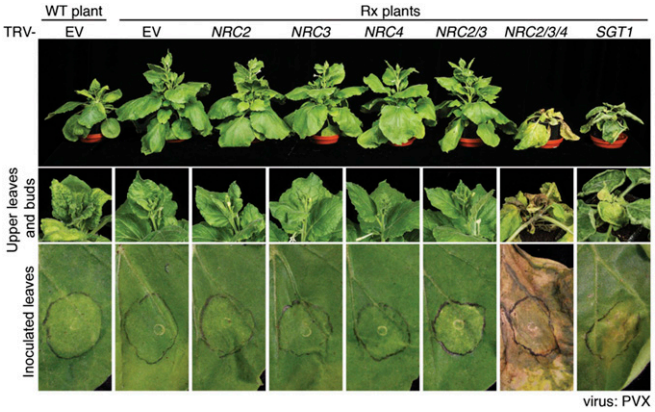

Fig. 3. Triple silencing of *NRC2*, *NRC3*, and *NRC4* compromised Rx-mediated extreme resistance to PVX. *NRC2*, *NRC3*, or *NRC4* was silenced individually or in combination in *Rx* transgenic plants by TRV. *SGT1* silencing, which compromises Rx-mediated resistance, was used as a control. The circles on the inoculated leaves indicate the area of PVX inoculation by agroinfection. Photographs were taken 2 wk after PVX inoculation.

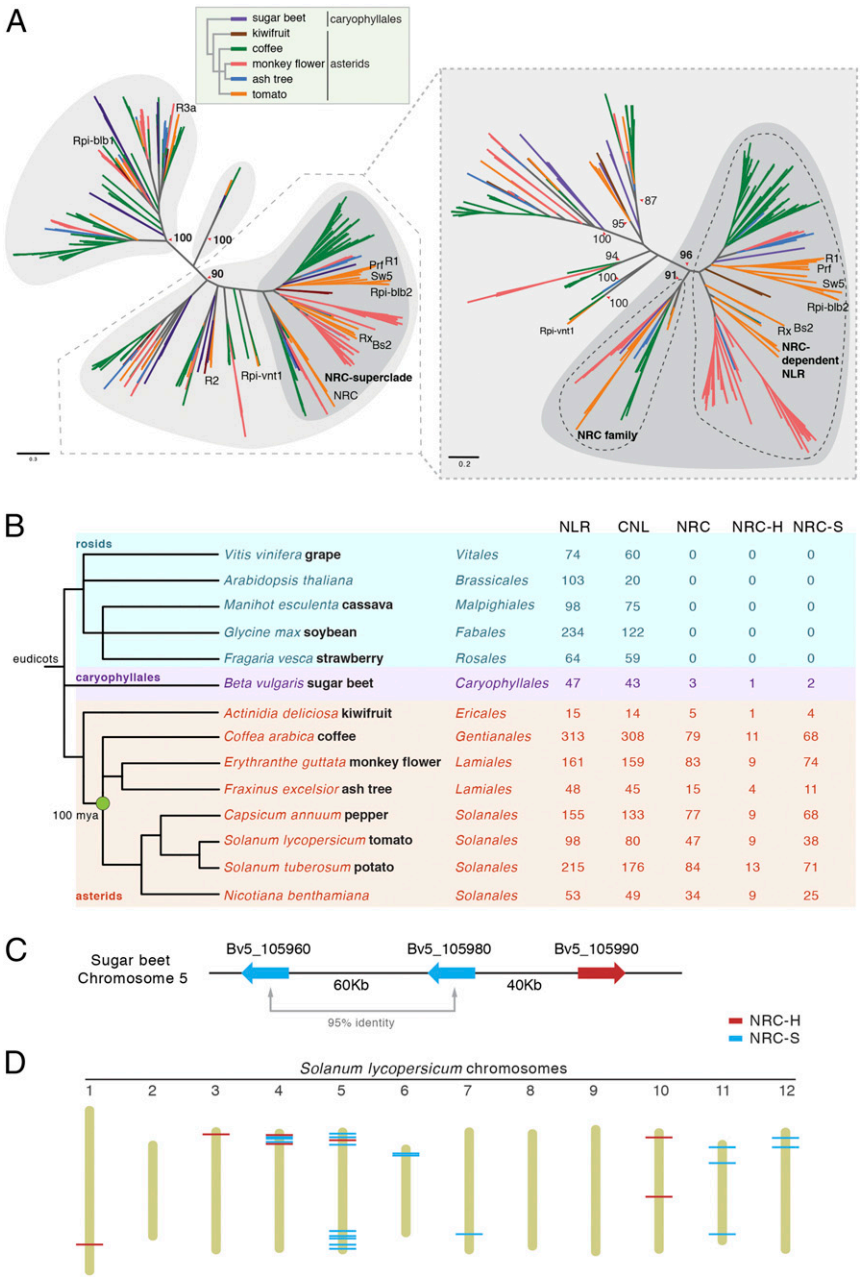

Fig. 4. NRC superclade emerged from an NLR pair over 100 Mya. (*A*) Phylogeny of CNL (CC-NLR) identified from asterids (kiwifruit, coffee, monkey flower, ash tree, and tomato) and caryophyllales (sugar beet). Only sequences with complete NLR features predicted by NLR-parser were included in the analysis. Sequences identified from different species are marked with different colors as indicated. The bootstrap supports of the major nodes are indicated. The phylogenetic tree (*Right*) which includes only sequences from the indicated lineages (*Left*), shows that the NRC sequences form a well-supported superclade that occurs in asterids and caryophyllales. The scale bars indicate the evolutionary distance in amino acid substitution per site. Details of the full phylogenetic tree can be found in *SI Appendix*, Figs. S21 and S22. (*B*) Summary of phylogeny and number of NLRs identified in different plant species. A phylogenetic tree of plant species was generated using phyloT based on National Center for Biotechnology Information taxon identification numbers. Numbers of NLRs identified in each category were based on NLR-parser and the phylogenetic trees in *A* and *SI Appendix*, Figs. S18–S22. NRC, NRC superclade; NRC-H, NRC family (helper NLR); NRC-S, NRC-dependent NLR (sensor NLR). (*C*) Schematic representation of the NRC gene cluster on sugar beet chromosome 5. The two NRC-S paralogs are marked in blue, and the NRC-H gene is marked in red. (*D*) Physical map of NRC superclade genes on tomato chromosomes. The NRC-S paralogs are marked in blue, and the NRC-H paralogs are marked in red. Detailed information of the physical map is available in *SI Appendix*, Fig. S23.

SI Appendix, Fig. S13). This phenotype, known as trailing necrosis, reflects spread of the virus when Rx-mediated extreme resistance is compromised (27). We further validated systemic spread of the virus by detecting accumulation of GFP driven by the subgenomic promoter of PVX (*SI Appendix*, Fig. S14). Indeed, silencing-resilient *NRC2*, *NRC3*, and *NRC4* individually complemented the loss of resistance to PVX in triple *NRC*-silenced plants confirming their functional redundancy in disease resistance (*SI Appendix*, Fig. S15). This and previous results indicate that the three NRC proteins display varying degrees of redundancy and specificity toward the nine NLRs, revealing a complex immune signaling network (*SI Appendix*, Fig. S16).

Tomato NRCs Rescue NRC-Dependent Cell Death in *N. benthamiana*. Most of the sensor NLRs in the NRC network we tested here originate from wild *Solanum* species, and yet confer disease resistance when introduced into tomato (*Solanum lycopersicum*), potato (*Solanum tuberosum*), and *N. benthamiana* (*SI Appendix*, Table S1). This observation prompted us to test whether NRCs from tomato display the same sensor NLR spectrum as their *N. benthamiana* orthologs. Largely consistent with the network we proposed, expression of tomato *NRCs* rescued cell death when their orthologous *N. benthamiana NRCs* were silenced (*SI Appendix*, Figs. S16 and S17). However, tomato *NRC3* rescued Rpi-blb2/Mi–mediated cell death in *NRC4*-silenced *N. benthamiana*, unlike *N. benthamiana* NRC3 (*SI Appendix*, Figs. S11 and S17*A*). In addition, tomato *NRC2* only weakly rescued Prf-mediated cell death in *NRC2/3*-silenced *N. benthamiana* (*SI Appendix*, Fig. S17*B*), and tomato *NRC4* only weakly rescued Sw5-mediated cell death in *NRC2/3/4*-silenced *N. benthamiana* (*SI Appendix*, Fig. S17*C*). We conclude that the NRC network structure may have evolved differently in the various Solanaceae species since divergence from their last common ancestor. Further studies on sequence polymorphisms and the sensor NLR spectrum of different NRC homologs should help reveal how helper-sensor specificity is determined in an NLR signaling network.

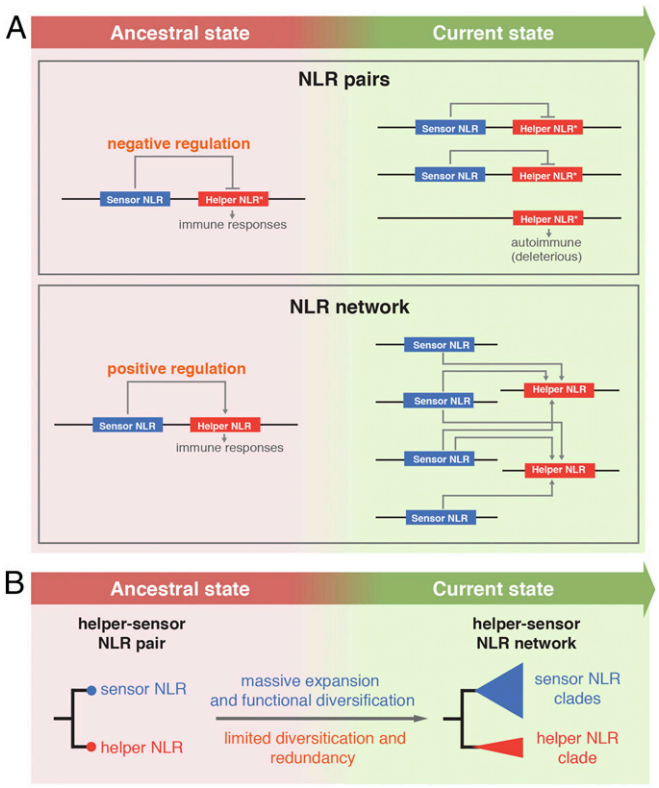

Fig. 5. Constraints and plasticity in plant NLR evolution. (*A*) NLR evolution must be constrained by its mode of action. Some NLR pairs are known to operate by negative regulation with the helper NLR exhibiting autoimmunity (NLR*) and the sensor NLR acting as a helper inhibitor. In such cases, expansion of the pair will be constrained throughout evolution due to the genetic load caused by autoimmunity. In contrast, NLRs that function through a different mechanism (e.g., positive regulation of the NLR helper by the sensor) will be less constrained to evolve into networks beyond genetically linked pairs of NLRs. (*B*) Model of the expansion of the NRC superclade from an ancestral pair of NLRs. The NRC-helper clade has expanded to create genetic redundancy, and thus flexibility for the sensor NLR to evolve rapidly. However, due to the constraints for mediating conserved downstream signaling, the diversification of the helper clade is likely to remain limited. In contrast, the NRC-sensor homologs have evolved into several diversified clades to detect proteins from a diversity of pathogens. This network system with redundant helper NLR may provide a framework for rapid evolution of plant NLR-triggered immunity to counteract fast-evolving pathogens.

The NRC Superclade Emerged from an NLR Pair Over 100 Mya. Our observation that NRC proteins and their NLR mates are related in the phylogeny of solanaceous CNL proteins (*SI Appendix*, Fig. S5) prompted us to reconstruct the evolutionary history of the NRC superclade. Higher order phylogenetic analyses of complete CNL repertoires from representative plant taxa revealed that the NRC superclade is missing in rosids but present in the examined representatives of caryophyllales (sugar beet) and asterids (kiwifruit, coffee, monkey flower, ash tree, and Solanaceae species) (Fig. 4 *A* and *B* and *SI Appendix*, Figs. S18–S22). Interestingly, sugar beet and kiwifruit, the early branching species, have only a single protein that groups with the NRC family (referred to as NRC-H), along with two and four NLRs, respectively, that cluster with the NRC-dependent NLRs (referred to as NRC-S) (Fig. 4 *A* and *B* and *SI Appendix*, Fig. S22). The dramatic expansion of the NRC superclade started before the divergence of Gentianales (coffee) from other asterids around 100 Mya to account for over one-half of all NLRs in some of the species (44) (Fig. 4*B*). We postulate that the NRC superclade has probably evolved from an ancestral pair of genetically linked NLR genes, as in sugar beet, to duplicate and expand throughout the genomes of asterid species into a complex genetic network that confers immunity to a diversity of plant pathogens (Fig. 4 *C* and *D* and *SI Appendix*, Fig. S23).

What Forces Drive the Evolution of an NLR Pair into a Network? NRC family members appear to be a convergent signaling point for a large repertoire of NLRs. The observation that sugar beet (caryophyllales) has only three closely linked NLR genes belonging to the NRC superclade supports the hypothesis that NRC and its mates evolved from a genetically linked NLR pair. Models of NLR evolution suggest that once an NLR gene translocates to an unlinked locus, it becomes more likely to diversify into a new function than when it remains in a gene cluster (34). Thus, expansion of the NRC superclade from a genetically linked pair to a genetically unlinked network may have been a key evolutionary step that accelerated functional diversification to confer immunity to multiple pathogens and pests. However, NLR evolution must be constrained by its mode of action. Recent studies on genetically linked NLR pairs, such as RPS4/RRS1 and RGA4/RGA5, suggested that the encoded proteins activate immune signaling through release of negative regulation (37, 38). The selective pressures shaping the evolution of NLR pairs that operate by negative regulation can be expected to limit their expansion due to the genetic load caused by autoimmunity (Fig. 5*A*). Autoactive NLR helpers and their negative regulators are expected to function as a single unit (supergene) and are likely to remain genetically linked over evolution. In contrast, NRC and NRC-dependent NLR proteins appear to function through a mechanism that accommodates evolutionary plasticity beyond genetically linked pairs of NLR proteins. We propose that NRC and NRC-dependent NLR proteins act through positive regulation rather than suppression of autoactivity (Fig. 5*A*). Such a mode of action would have enabled massive duplication and functional diversification without accumulation of deleterious effects. Interestingly, recent studies have shown that mismatched NLRs, which probably operate through positive regulation, trigger autoimmunity leading to hybrid necrosis, adding another layer of complexity in NLR evolution (43, 45). Future studies on how NRC and NRC-dependent NLR proteins function should shed light on the mechanistic detail of how this NRC network mediates immune responses and disease resistance. Of particular interest, it would be important to determine how the genetically defined sensor and helper activities of NRCs and their mates translate into biochemical models and the extent to which these proteins associate into a signaling complex.

NLR Networks Increase Robustness of the Plant Immune System. Genetic redundancy is known to enhance robustness and evolvability of biological systems (46–48). The emergence of genetic redundancy ultimately leads to a network architecture, a general feature of many complex biological processes (49). Traits under strong natural selection, such as immunity, should benefit from the increase in evolutionary plasticity and tolerance to environmental disturbance conferred by gene duplications (50, 51). Redundant helper NLRs may therefore provide a stepping stone for rapid expansion and functional diversification of their matching sensor NLRs to counteract rapidly evolving pathogens (Fig. 5*B*). Interestingly, a recent analysis of NLR evolutionary patterns in Solanaceae revealed that the NRC clade [termed CNL-G8 by Seo et al. (31)] stands out as having only a few recent duplications that occurred after speciation of pepper, tomato, and potato. This finding is consistent with the view that, unlike their NLR mates, NRCs may not be directly involved in detecting pathogens and are diversifying at a slower pace. NRCs may also be constrained by their central function in immune signaling as nodes in a signaling network with a bow-tie architecture (i.e., diversity of inputs converging on a few core elements). Similar bow-tie network architectures have also been described in immunity in other systems, such as animal Toll-like receptors, in which diversified receptors sense a wide variety of microbial molecules with a few core elements playing signaling roles in mediating downstream output (52). We propose that the NRC network is a powerful system to study robustness, redundancy, and specificity of an NLR immune

signaling network within a solid evolutionary framework. Harnessing the processes that underpin NLR network structure and function would open up new approaches for developing disease-resistant crops.

Materials and Methods

Hypersensitive Cell Death Assays. Hypersensitive cell death assays were performed using *Agrobacterium*-mediated transient gene expression. Detailed procedures and information on constructs used in this study are provided in *SI Appendix, SI Materials and Methods*.

Disease Resistance Assays. Rpi-blb2, Rpi-blb1, R3a, Pto/Prf, and Rx transgenic *N. benthamiana* plants were used for disease resistance assays. R1 was transiently expressed on leaves of *N. benthamiana* for disease resistance assays. Detailed procedures on disease resistance assays to *P. infestans*, *P. syringae*, and PVX are provided in *SI Appendix, SI Materials and Methods*.

Virus-Induced Gene Silencing and Complementation. Virus-induced gene silencing (VIGS) was performed in *N. benthamiana* as described in *SI Appendix, SI Materials and Methods*. For complementation, silencing-resilient *NRC* variants were generated by introducing synonymous substitutions into the targeted codons. Detail procedures for VIGS, construction of VIGS vectors, RT-PCR, and design of complementation are described in *SI Appendix, SI Materials and Methods*.

Phylogenetic Analysis. Sequences of NLR were aligned using Clustal OMEGA or MAFFT, and then manually edited in MEGA7. The sequences of the nucleotide-binding (NB) domains were used for generating a maximum-likelihood tree in MEGA7. NLR-parser was used to identify the NLR sequences from the databases of different plant species. Detail procedures are provided in *SI Appendix, SI Materials and Methods*.

ACKNOWLEDGMENTS. We thank Oliver Furzer, Jonathan Jones, John Rathjen, Sebastian Schornack, Geert Smant, Brian Staskawicz, Frank Takken, Vivianne Vleeshouwers, and Cyril Zipfel for providing materials and technical support. We thank Yasin Dagdas, Lida Derevnina, Esther van der Knaap, Benjamin Petre, Silke Robatzek, and Erin Zess for helpful suggestions. This project was funded by the Gatsby Charitable Foundation, Biotechnology and Biological Sciences Research Council, and European Research Council.

1. Dangl JL, Horvath DM, Staskawicz BJ (2013) Pivoting the plant immune system from dissection to deployment. *Science* 341:746–751, and erratum (2013) 341:1175.
2. von Moltke J, Ayres JS, Kofoed EM, Chavarría-Smith J, Vance RE (2013) Recognition of bacteria by inflammasomes. *Annu Rev Immunol* 31:73–106.
3. Dodds PN, Rathjen JP (2010) Plant immunity: Towards an integrated view of plant-pathogen interactions. *Nat Rev Genet* 11:539–548.
4. Jacob F, Vernaldi S, Maekawa T (2013) Evolution and conservation of plant NLR functions. *Front Immunol* 4:297.
5. Clark RM, et al. (2007) Common sequence polymorphisms shaping genetic diversity in *Arabidopsis thaliana*. *Science* 317:338–342.
6. McHale L, Tan X, Koehl P, Michelmore RW (2006) Plant NBS-LRR proteins: Adaptable guards. *Genome Biol* 7:212.
7. Win J, et al. (2012) Effector biology of plant-associated organisms: Concepts and perspectives. *Cold Spring Harb Symp Quant Biol* 77:235–247.
8. Bonardi V, et al. (2011) Expanded functions for a family of plant intracellular immune receptors beyond specific recognition of pathogen effectors. *Proc Natl Acad Sci USA* 108:16463–16468.
9. Cesari S, Bernoux M, Moncuquet P, Kroj T, Dodds PN (2014) A novel conserved mechanism for plant NLR protein pairs: The "integrated decoy" hypothesis. *Front Plant Sci* 5:606.
10. Eitas TK, Dangl JL (2010) NB-LRR proteins: Pairs, pieces, perception, partners, and pathways. *Curr Opin Plant Biol* 13:472–477.
11. Wu CH, Belhaj K, Bozkurt TO, Birk MS, Kamoun S (2016) Helper NLR proteins NRC2a/b and NRC3 but not NRC1 are required for Pto-mediated cell death and resistance in *Nicotiana benthamiana*. *New Phytol* 209:1344–1352.
12. Särkinen T, Bohs L, Olmstead RG, Knapp S (2013) A phylogenetic framework for evolutionary study of the nightshades (Solanaceae): A dated 1000-tip tree. *BMC Evol Biol* 13:214.
13. van Ooijen G, van den Burg HA, Cornelissen BJC, Takken FLW (2007) Structure and function of resistance proteins in solanaceous plants. *Annu Rev Phytopathol* 45:43–72.
14. Vleeshouwers VGAA, et al. (2011) Understanding and exploiting late blight resistance in the age of effectors. *Annu Rev Phytopathol* 49:507–531.
15. Jo KR, et al. (2014) Development of late blight resistant potatoes by cisgene stacking. *BMC Biotechnol* 14:50.
16. Haverkort AJ, Struik PC, Visser RGF, Jacobsen E (2009) Applied biotechnology to combat late blight in potato caused by *Phytophthora infestans*. *Potato Res* 52:249–264.
17. Milligan SB, et al. (1998) The root knot nematode resistance gene *Mi* from tomato is a member of the leucine zipper, nucleotide binding, leucine-rich repeat family of plant genes. *Plant Cell* 10:1307–1319.
18. Nombela G, Williamson VM, Muñiz M (2003) The root-knot nematode resistance gene Mi-1.2 of tomato is responsible for resistance against the whitefly *Bemisia tabaci*. *Mol Plant Microbe Interact* 16:645–649.
19. Rossi M, et al. (1998) The nematode resistance gene Mi of tomato confers resistance against the potato aphid. *Proc Natl Acad Sci USA* 95:9750–9754.
20. Tai TH, et al. (1999) Expression of the *Bs2* pepper gene confers resistance to bacterial spot disease in tomato. *Proc Natl Acad Sci USA* 96:14153–14158.
21. Brommonschenkel SH, Frary A, Frary A, Tanksley SD (2000) The broad-spectrum tospovirus resistance gene *Sw-5* of tomato is a homolog of the root-knot nematode resistance gene *Mi*. *Mol Plant Microbe Interact* 13:1130–1138.
22. van der Vossen EA, et al. (2000) Homologues of a single resistance-gene cluster in potato confer resistance to distinct pathogens: A virus and a nematode. *Plant J* 23:567–576.
23. Bendahmane A, Kanyuka K, Baulcombe DC (1999) The *Rx* gene from potato controls separate virus resistance and cell death responses. *Plant Cell* 11:781–792.
24. Balmuth A, Rathjen JP (2007) Genetic and molecular requirements for function of the Pto/Prf effector recognition complex in tomato and *Nicotiana benthamiana*. *Plant J* 51:978–990.
25. Gutierrez JR, et al. (2010) Prf immune complexes of tomato are oligomeric and contain multiple Pto-like kinases that diversify effector recognition. *Plant J* 61:507–518.
26. Mucyn TS, et al. (2006) The tomato NBARC-LRR protein Prf interacts with Pto kinase in vivo to regulate specific plant immunity. *Plant Cell* 18:2792–2806.
27. Tameling WIL, Baulcombe DC (2007) Physical association of the NB-LRR resistance protein Rx with a Ran GTPase-activating protein is required for extreme resistance to *Potato virus X*. *Plant Cell* 19:1682–1694.
28. Tameling WI, et al. (2010) RanGAP2 mediates nucleocytoplasmic partitioning of the NB-LRR immune receptor Rx in the Solanaceae, thereby dictating Rx function. *Plant Cell* 22:4176–4194.
29. Sacco MA, Mansoor S, Moffett P (2007) A RanGAP protein physically interacts with the NB-LRR protein Rx, and is required for Rx-mediated viral resistance. *Plant J* 52:82–93.
30. Shao ZQ, et al. (2016) Large-scale analyses of angiosperm nucleotide-binding site-leucine-rich repeat genes reveal three anciently diverged classes with distinct evolutionary patterns. *Plant Physiol* 170:2095–2109.
31. Seo E, Kim S, Yeom SI, Choi D (2016) Genome-wide comparative analyses reveal the dynamic evolution of nucleotide-binding leucine-rich repeat gene family among Solanaceae plants. *Front Plant Sci* 7:1205.
32. Michelmore RW, Meyers BC (1998) Clusters of resistance genes in plants evolve by divergent selection and a birth-and-death process. *Genome Res* 8:1113–1130.
33. Chen Q, Han Z, Jiang H, Tian D, Yang S (2010) Strong positive selection drives rapid diversification of R-genes in Arabidopsis relatives. *J Mol Evol* 70:137–148.
34. Leister D (2004) Tandem and segmental gene duplication and recombination in the evolution of plant disease resistance gene. *Trends Genet* 20:116–122.
35. van der Vossen EAG, et al. (2005) The *Rpi-blb2* gene from *Solanum bulbocastanum* is an *Mi-1* gene homolog conferring broad-spectrum late blight resistance in potato. *Plant J* 44:208–222.
36. Oh SK, et al. (2009) In planta expression screens of *Phytophthora infestans* RXLR effectors reveal diverse phenotypes, including activation of the *Solanum bulbocastanum* disease resistance protein Rpi-blb2. *Plant Cell* 21:2928–2947.
37. Williams SJ, et al. (2014) Structural basis for assembly and function of a heterodimeric plant immune receptor. *Science* 344:299–303.
38. Césari S, et al. (2014) The NB-LRR proteins RGA4 and RGA5 interact functionally and physically to confer disease resistance. *EMBO J* 33:1941–1959.
39. Vossen JH, et al. (2016) The *Solanum demissum R8* late blight resistance gene is an *Sw-5* homologue that has been deployed worldwide in late blight resistant varieties. *Theor Appl Genet* 129:1785–1796.
40. Ballvora A, et al. (2002) The *R1* gene for potato resistance to late blight (*Phytophthora infestans*) belongs to the leucine zipper/NBS/LRR class of plant resistance genes. *Plant J* 30:361–371.
41. Collier SM, Hamel LP, Moffett P (2011) Cell death mediated by the N-terminal domains of a unique and highly conserved class of NB-LRR protein. *Mol Plant Microbe Interact* 24:918–931.
42. Andolfo G, et al. (2014) Defining the full tomato NB-LRR resistance gene repertoire using genomic and cDNA RenSeq. *BMC Plant Biol* 14:120.
43. Tran DTN, et al. (2017) Activation of a plant NLR complex through heteromeric association with an autoimmune risk variant of another NLR. *Curr Biol* 27:1148–1160.
44. Wikström N, Kainulainen K, Razafimandimbison SG, Smedmark JEE, Bremer B (2015) A revised time tree of the asterids: Establishing a temporal framework for evolutionary studies of the coffee family (Rubiaceae). *PLoS One* 10:e0126690.
45. Chae E, et al. (2014) Species-wide genetic incompatibility analysis identifies immune genes as hot spots of deleterious epistasis. *Cell* 159:1341–1351.
46. Fares MA (2015) The origins of mutational robustness. *Trends Genet* 31:373–381.
47. Kitano H (2004) Biological robustness. *Nat Rev Genet* 5:826–837.
48. Whitacre JM (2012) Biological robustness: Paradigms, mechanisms, and systems principles. *Front Genet* 3:67.
49. Nowak MA, Boerlijst MC, Cooke J, Smith JM (1997) Evolution of genetic redundancy. *Nature* 388:167–171.
50. Salathé M, Soyer OS (2008) Parasites lead to evolution of robustness against gene loss in host signaling networks. *Mol Syst Biol* 4:202.
51. Zhang R, Murat F, Pont C, Langin T, Salse J (2014) Paleo-evolutionary plasticity of plant disease resistance genes. *BMC Genomics* 15:187.
52. Oda K, Kitano H (2006) A comprehensive map of the toll-like receptor signaling network. *Mol Syst Biol* 2:2006.0015.

Supporting Information

SI Materials and Methods

Growth condition of *Nicotiana benthamiana* lines. Wild type and transgenic *N. benthamiana* lines were grown in a controlled growth chamber with temperature 22-25°C, humidity 45-65% and 16/8-h light/dark cycle. Details of transgenic *N. benthamiana* lines expressing different NLR genes are listed in Table S2.

Cloning of *NRC2*, *NRC3* and *NRC4.* Cloning of *NRC2* (*NRC2a* and *NRC2b*, simplified as *NRC2*) and *NRC3* were described previously (1). NRC2a and NRC2b shares around 98% sequence identity and are functionally equivalent in *Prf*-mediated responses (1). Thus, only sequence of NRC2a was used in comparisons performed in Fig. S7. Sequences of primers used in cloning of NRC4 variants are listed in Table S3. *NRC4* was amplified from *N. benthamiana* cDNA and cloned into pENTR/D-TOPO (Invitrogen). This plasmid was then used for further subcloning of NRC4 into pCR8/GW/D-TOPO (Invitrogen) as a level 0 module for follow-up Golden Gate cloning (2). GFP:NRC4 was generated by Golden Gate assembly with pICSL12008 (35S promoter, The Sainsbury Laboratory (TSL) SynBio), pICSL30006 (GFP, TSL SynBio), pCR8-NRC4, pICH41432 (OCS terminator) into binary vector pICH86966 (2, 3). To make a level 0 module for NRC4 C-terminal tagging, the stop codon was removed in pCR8-NRC4 to generate pCR8-NRC4-ns. NRC4:myc was generated by assembling pCR8-NRC4-ns with pICSL50010 (4xmyc, TSL SynBio) in pICH86988**.** The synthetic fragment (1-272bp) of *NRC4* was designed manually to introduce synonymous substitution in every codon possible. The fragment was synthesized by GENEWIZ (South Plainfield, NJ, USA) and then subcloned into binary vector pICH86988 together with the remaining part of NRC4 (273-2646bp) by Golden Gate cloning to generate a full-length NRC4 variant. To confirm the accumulation of proteins in the wild type or *NRC4*-silenced plant background, a GFP tag was fused to the N-terminal of NRC4 and cloned into pICH86966. Three days after agroinfiltration in control or *NRC4*-silenced leaves, total plant proteins were extracted, and analyzed using western blot analyses. Anti-GFP (A11122, Invitrogen) and anti-rabbit antibody conjugated to horseradish peroxidase

(Sigma-Aldrich) were used as primary and secondary antibodies. Confirmation of accumulation of synthetic NRC2 and NRC3 were described previously (1). Fusion of GFP to the N-terminus of NRCs impair the activities of NRCs. Thus, GFP:NRC variants were used only for confirming protein accumulation as indicated. Functional analyses of NRCs were performed with untagged variants, while C-terminally myc tagged variants display consistent results as untagged variants in the complementation assays.

DNA sequences and accession numbers of NRC homologs. Sequences of *NRC* homologs used in this study can be found in the Solanaceae Genomics Network (SGN) or GenBank/EMBL databases with the following accession numbers: *Nb*NRC2 (NbS00018282/KT936525, NbS00026706/KT936526), *Nb*NRC3 (NbS00011087), *Nb*NRC4 (NbS00002971, NbS00016103), *Sl*NRC2 (Solyc10g047320), *Sl*NRC3 (XP_004238948.1, Solyc05g009630), *Sl*NRC4 (Solyc04g007070).

Site-directed mutagenesis of Rpi-blb2 and NRC4. To determine whether an intact p-loop is essential for the function of Rpi-blb2 and NRC4, a lysine (K) to arginine (R) mutation was introduced into the p-loops of both proteins independently. Primers listed in Table S4 were used for introducing the mutations by inverse PCR with Phusion High-Fidelity DNA Polymerase (Thermo). The mutated variants were verified by sequencing, and then subcloned into pK7WGF2 (for GFP:Rpi-blb2) or pICH86966 (for NRC4:myc). To confirm the accumulation of the encoded proteins, wild type and mutated GFP:Rpi-blb2 or NRC4:myc were independently transiently expressed in *N. benthamiana* leaves. Samples were collected 3 days after infiltration for immunoblot analysis with anti-GFP (A11122, Invitrogen), or anti-myc (A-14, Santa Cruz Biotechnology) antibodies.

Virus induced gene silencing (VIGS) of *NRC* homologs. VIGS was performed in *N. benthamiana* as described by Liu *et al.* (2002). Suspensions of *Agrobacterium tumefaciens* strain GV3101 harboring TRV RNA1 (pYL155) and TRV RNA2 (pYL279) (4), with corresponding fragments from indicated genes, were mixed in a 2:1 ratio in infiltration buffer (10mM MES, 10mM $MgCl_2$, and 150μM acetosyringone, pH5.6) to a

final OD_{600} of 0.3. Two-week-old *N. benthamiana* plants were infiltrated with *A. tumefaciens* for VIGS assays, upper leaves were used two to three weeks later for further agroinfiltrations. To silence *NRC4*, a 395bp fragment from 5'UTR (-123) to coding region (+272) was cloned into pYL279. For *NRC2/3/4* triple silencing, fragments of *NRC4* (1-272), *NRC3* (1-$_{295}$) and *NRC2a* (1-285) were synthesized as one unit by GENEWIZ and subcloned into pYL279. The silencing constructs for *NRC2, NRC3 and SGT1* were described previously (1, 5).

PCR and RT-PCR of *NRC* homologs. DNeasy Plant Mini Kit (Qiagen) was used for extracting genomic DNA from *N. benthamiana* leaves according to manufacturer's instruction. To test PCR primer pairs for amplification of NRC family members, 5ng of genomic DNA was used in a 20μL reaction. Plant total RNA was extracted using RNeasy Mini Kit (Qiagen). DNA contamination in the RNA sample was removed by on-column digestion with RNase-Free DNase Set (Qiagen). Subsequently, 2μg of each RNA sample was subject to first strand cDNA synthesis using Ominiscript RT Kit (Qiagen). PCR and semi-quantitative RT-PCR were performed using DreamTaq (Thermo Scientific) with 25 to 35 amplification cycles followed by electrophoresis with 2% agarose gel stained with ethidium bromide. The primers used in the RT-PCR and PCR are listed in Table S4.

***Rpi-blb2*-mediated resistance.** Assays of disease resistance to *P. infestans* were performed by applying droplets of zoospore suspension on detached leaves as described previously (6). *NRC* homologs were silenced by VIGS in *Rpi-blb2* transgenic *N. benthamiana* lines as described above. Three weeks after TRV inoculation, mature leaves were detached and used for disease resistance assays. The *P. infestans* 88069 zoospore suspension was prepared according to the methods reported by Song et al. (2009) and adjusted to 100 zoospores/μL. To inoculate *P. infestans* on detached leaves, 10μL drops of zoospore were applied to the abaxial side of the leaves. The inoculated leaves were kept in a moist chamber at room temperature (21-24°C) for 4 days, and imaged under UV light for visualization of the lesions. For each biological replicate, 4 leaves from 2 independent VIGSed plants were used and 6 spots on each leaf were inoculated with the pathogen. Experiments were repeated 3 times. For the complementation assay,

suspensions of *A. tumefaciens* containing empty vector or expression construct of synthetic *NRC4* (untagged) were adjusted to OD_{600} of 0.6 and infiltrated into the leaves one day before pathogen inoculation. We observed that agroinfiltration delayed the progress of *P. infestans* infection lesion development. Hence, the leaves were imaged 5 days after inoculation. To check the accumulation of Rpi-blb2 in *NRC4*-silenced plants, RFP:Rpi-blb2 was transiently expressed in control and *NRC4*-silenced leaves by agroinfiltration. Leaf samples were collected three days after infiltration for immunoblot with anti-GFP antibody (A11122, Invitrogen).

***R1*-mediated resistance.** For analysis of R1-mediated resistance, suspensions of *A. tumefaciens* containing empty vector or R1 expression construct (untagged) were adjusted to OD_{600} of 0.5 and then infiltrated into *NRC4*-silenced or control *N. benthamiana*. Half of each leaf was infiltrated with *A. tumefaciens* containing empty vector plasmid, whereas the other half of the leaf was infiltrated with *A. tumefaciens* containing R1 expression vector. Experiments were repeated four times with 21 inoculation sites per condition in each biological replicate. *P. infestans* T30-4 was used for R1-mediated resistance assay. The zoospore suspension was prepared as described above and adjusted to 200 zoospores/μL. For the complementation assay, R1 was co-expressed with empty vector or synthetic *NRC4* in *NRC4*-silenced or control *N. benthamiana* on day before pathogen inoculation.

***Rpi-blb1* and *R3a*-mediated resistance.** *NRC* homologs were silenced using VIGS as described above in *Rpi-blb1* and *R3a* transgenic *N. benthamiana*. *Rpi-blb2* transgenic plants were used in parallel as controls for silencing and successful pathogen inoculation. *SGT1*-silencing was used as an additional control for this experiment as *SGT1* was demonstrated to be essential for the responses mediated by R3a and Rpi-blb1 in hypersensitive cell death assays. Three weeks after TRV inoculation, mature leaves of the plants were used for disease resistance assay according to the description above. *Rpi-blb2* and *Rpi-blb1* transgenic plants were inoculated with *P. infestans* 88069. However, *P. infestans* 88069 is homozygous for $AVR3a^{EM}$, which avoids *R3a*-medaited detection (7, 8). Therefore, *P. infestans* NL00228, which is homozygous for $AVR3a^{KI}$ and is not

virulent on R3a plants, was used for inoculation on R3a transgenic *N. benthamiana* (7, 8). The experiments were repeated three times with 24 inoculation sites per condition in each biological replicate. Pictures were taken 4 days after pathogen inoculation for the analysis with *P. infestans* 88069 and 5 days after inoculation for the analysis with *P. infestans* NL00228.

Rx-mediated resistance. *NRC* homologs or *SGT1* were silenced by VIGS as described above in *Rx* transgenic *N. benthamiana*. Three weeks after TRV infection, *Potato virus X* (PVX, pGR106) was inoculated on the leaves through agroinfection as described previously (9). To generate PVX-GFP, a DNA fragment of GFP was amplified from pK7WGF2 and cloned into pGR106. Suspensions of *A. tumefaciens* carrying the PVX vector pGR106 or pGR106-GFP were adjusted to OD_{600} of 0.005 and then infiltrated into mature leaves of Rx *N. benthamiana*. This concentration of *A. tumefaciens* only causes infection of few cells in the infiltrated area and thus no visible necrotic lesion could be observed when the resistance response is strong and rapid, i.e. extreme resistance. The infiltrated area was then circled with a marker pen. Trailing necrotic lesions, as a sign of compromised resistance (9, 10), were observed at inoculated leaves of the *NRC2/3/4*-silenced *Rx* plants starting from 10 days after inoculation, and the necrotic lesion spread gradually to the upper leaves and apical buds. Photos were taken at 15 days after inoculation under daylight or UV light. Samples from the upper leaves were collected at 15 days after inoculation and analyzed by immunoblot to detect GFP accumulation. To check the accumulation of Rx in *NRC2/3/4* or *SGT1* silenced *N. benthamiana*, leaf samples were collected at three weeks after TRV inoculation and anti-HA antibody (3F10, Roche) was used as primary antibody for immunoblot analysis. For complementation assays with synthetic NRC variants, we took advantage of the toothpick inoculation method (11), which allowed us to examine the spread of trailing necrotic lesions from the inoculated spots. One day before PVX toothpick inoculation, synthetic NRC variants (untagged) were expressed by agroinfiltration on leaves of *Rx* plants silenced with *NRC2/3/4*. Toothpicks were dipped into the culture of *A. tumefaciens* harboring PVX-GFP vector and then used to pierce small holes in the leaves of *N. benthamiana*. Photos were taken at 10 days after PVX inoculation, and the size of the

lesions were measured in ImageJ. Scatterplot of the lesion size was generated with R, using ggplot2 package and script published previously (12). A cork borer (0.9 cm^2) was used to collect leaf discs from the inoculation sites for immunoblot analysis.

Prf/Pto-mediated resistance. VIGS was used to silence *NRC2, NRC3* and *NRC4* in both wild type and *Pto/Prf* transgenic (R411B) *N. benthamiana* plants (13). Bacteria growth assays were performed as previously described with minor modifications (13). The *Pseudomonas syringae* pv. *tomato* DC3000 *ΔhopQ1-1* culture (14) was adjusted to OD_{600} of 0.2 and then diluted 10,000-fold with 10mM $MgCl_2$. Five-week-old *N. benthamiana* with VIGS control or *NRC*-silencing were inoculated with the bacterial culture using needleless syringe. Four replicate plants were sampled using 0.33cm^2 cork borer at each time point. The samples were independently homogenized in 10 mM $MgCl_2$ for serial dilution and plating. Experiments were repeated three times with similar results.

Expression constructs used in cell death assays. NLR immune receptor *R1* was amplified from genomic DNA of *Solanum demissum* with primers listed in Table S5, and then cloned into pK7WG2 using Gateway cloning kit (Invitrogen). *AVR1* was amplified from genomic DNA of *P. infestans* T30-4 with primers listed in Table S5 and then cloned into pK7WGF2 by using Gateway cloning kit (Invitrogen). Sw5b (NCBI_AAG31014.1) (15, 16) and NSm (NCBI_S58512.1) of TSWV (*Tomato spotted wilt virus*) (17, 18) were synthesized by GENEWIZ as Golden Gate level 0 modules and then subcloned into binary vector pICSL86977 (TSL SynBio). Tomato NLR *CNL-11990* was amplified from tomato (cv. Moneymaker) cDNA with the primers listed in Table S5 and then cloned into pICH86988 by Golden Gate cloning (2). Information of other constructs used for the cell death assays were summarized in Table S6.

Cell death assay in *NRC*-silenced *N. benthamiana.* Transient expression of NLR immune receptors and cognate effectors (or other proteins that induce cell death) were performed according to methods described previously (19). Briefly, four to five-week-old

N. benthamiana plants (i.e. two to three weeks after virus inoculation) were infiltrated with *A. tumefaciens* strains carrying the expression vector of different proteins indicated. *A. tumefaciens* suspensions were adjusted in infiltration buffer (10mM MES, 10mM $MgCl_2$, and 150μM acetosyringone, pH5.6) to the density indicated in Table S7. The hypersensitive cell death (HR) phenotype was scored at 7 dpi, according to a previously described scale, which was modified as from 0 (no necrosis observed) to 7 (confluent necrosis) (20).

Complementation assay of cell death. For the complementation assay of cell death in the *NRC*-silenced background (Fig. 1B, Fig. S6C, Fig. S11, Fig. S12, Fig. S17), suspensions of *A. tumefaciens* containing empty vector or expression construct of *NRC2, NRC3, or NRC4* variants (untagged) were adjusted to OD_{600} of 0.6 and co-infiltrated with the *A. tumefaciens* strains carrying the expression constructs indicated. Expression of original or synthetic *NRC2*, *NRC3* and *NRC4* without R/AVR combinations did not cause cell death (Fig. 1B) (1). The hypersensitive cell death (HR) was scored at 7 days after infiltration.

Phylogenetic analysis of the NRC family. Protein sequences of *N. benthamiana* NRC2, NRC3 and NRC4 were used to identify the homologs from predicted protein databases (*N. benthamiana* Genome v0.4.4 predicted protein, Tomato proteins ITAG release 2.40, and Potato ITAG release 1 predicted proteins) on the Solanaceae Genomics Network (SGN). The BLAST search results were compared to the previously published phylogeny (21), which revealed that the top hits of our BLASTP search results are all in the CNL-14 in the phylogenetic tree of solanaceous NLRs. We thus referred to this clade as the NRC family and combined all the candidate sequences in this clade for generating the phylogenetic tree. The protein sequences of the NRC family members were aligned using Clustal Omega and then manually edited in MEGA7 (22). The gaps in the alignment were deleted and only the NB-ARC domains were used for producing phylogenetic tree. The maximum-likelihood phylogenetic tree of NRC family was built using MEGA7 with

Jones-Taylor-Thornton (JTT) substitution model and bootstrap values based on 1000 iterations.

Phylogenetic analysis of solanaceous NLRs. NLR-parser (23) was used to identify the NLR sequences from the predicted protein databases of tomato, potato, *N. benthamiana*, and pepper downloaded from SGN (Tomato ITAG release 2.40, Potato PGSC DM v3.4, *N. benthamiana* Genome v0.4.4, Pepper cv CM334 v.1.55). The predicted NLR sequences, from NLR-parser, were classified into TNL and CNL, with complete or partial NLR features. Only CNL sequences with complete NLR features were used for further phylogenetic analysis. Sequences of characterized solanaceous NLR-type resistance proteins were included as reference for the clades described in literature (21). The sequences were aligned using MAFFT and then manually edited in MEGA7 (22, 24). The gaps in the alignment were deleted manually and only the NB-ARC domains were used for generating the phylogenetic tree. The maximum-likelihood tree of NRC family was produced using MEGA7 with JTT model and bootstrap values based on 100 iterations (Fig. S5). The resulting tree was then visualized using FigTree v1.2.4 (http://tree.bio.ed.ac.uk/software/figtree/). To simplify the phylogenetic tree, some branches were collapsed together into the same clade according to the bootstrap supports of the nodes.

Phylogenetic analysis of NLRs from rosids, asterids and caryophyllales. The protein databases of *Arabidopsis thaliana*, soybean (*Glycine max*), strawberry (*Fragaria vesca*), cassava (*Manihot esculenta*), grape (*Vitis vinifera*) and monkey flower (*Erythranthe guttata*, synonym: *Mimulus guttatus*) were downloaded from Phytozome v10 genomes (https://phytozome.jgi.doe.gov/pz/portal.html). Protein database of tomato was downloaded from SGN as indicated above. The databases of other species, which were not included in the Phytozome website, were downloaded from the sources indicated below: kiwifruit (http://bioinfo.bti.cornell.edu/cgi-bin/kiwi/home.cgi) (25), coffee (http://coffee-genome.org) (26), ash tree (http://www.ashgenome.org/home) (27) and sugar beet (http://bvseq.molgen.mpg.de/index.shtml, RefBeet-1.2) (28). NLR-parser was

used to identify the NLR sequences from the databases of different plant species. Only CNL sequences with complete NLR features were used for further phylogenetic analysis. The sequences were aligned by using MAFFT and manually edited in MEGA7 (22, 24). The gaps were removed and only the NB-ARC domains were used for phylogenetic analysis. To further confirm that the kiwifruit and sugar beet genomes contain only few sequences in the NRC-superclade compared to other asterid species, the sequences of these two species were further examined manually with BLASTP search and phylogenetic analyses. Consequently, two more sequences from sugar beet and one sequence from kiwifruit were added into the phylogenetic analysis with other asterids and caryophyllales species. The maximum-likelihood phylogenetic trees were generated using MEGA7 (22) with JTT model and bootstrap values based on 100 iterations (Fig. 4A, Fig. S18-22). The resulting tree was visualized using FigTree v1.2.4. Due to the numbers and complexity of NLRs identified from difference species, the phylogenetic analyses were first performed with comparing tomato (asterids) to rosids (Fig. S18, Fig. S19-20), and then comparing asterids to caryophyllales (Fig. 4A, Fig S21-22). The number of NLR homologs of the NRC family (NRC-H) and NRC-dependent NLR (NRC-S) were summarized in Fig 4B. Phylogeny of the plant species analyzed here was constructed using PhyloT (http://phylot.biobyte.de) based on NCBI taxonomy.

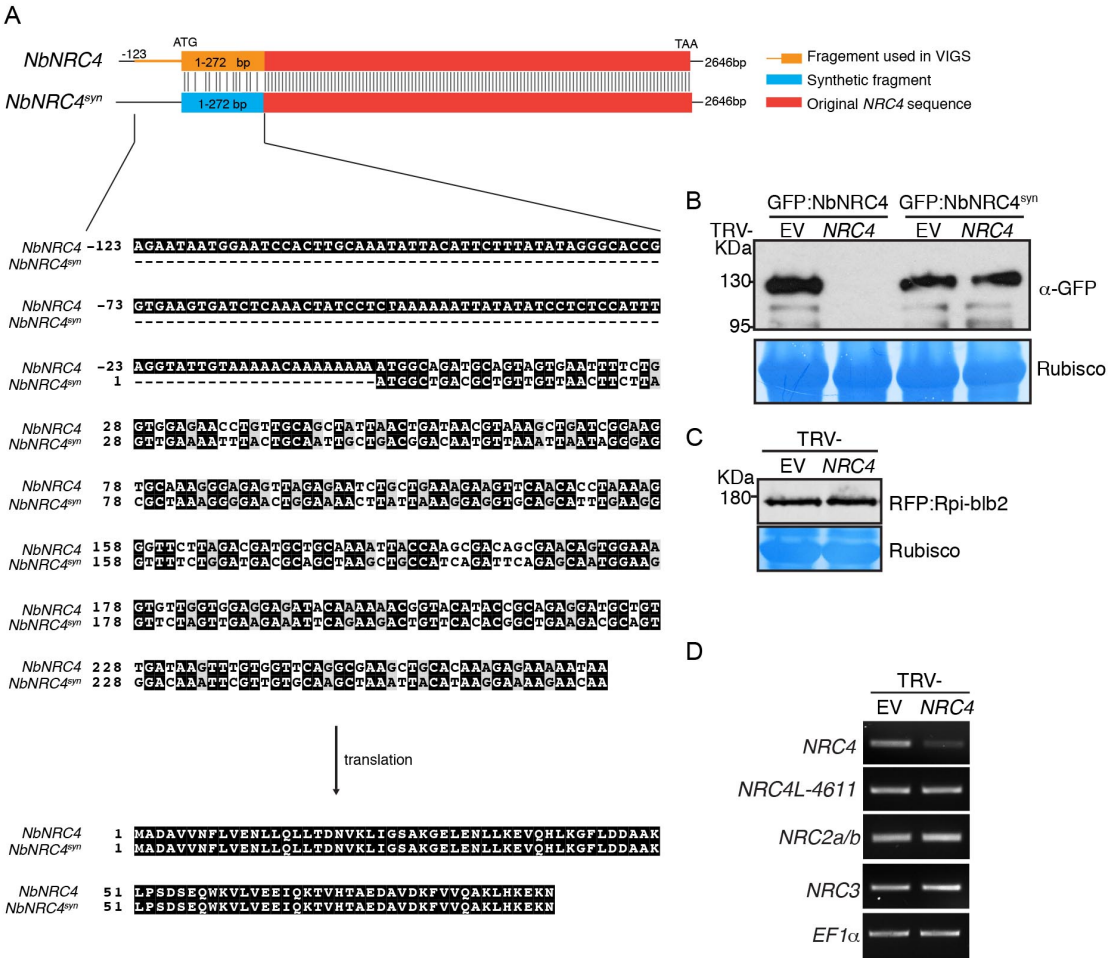

Fig. S1. Design of virus-induced gene silencing (VIGS) and complementation of *NRC4*

(**A**) Schematic representation of VIGS and complementation design. The region from -123bp to +272bp of *NRC4* was cloned into VIGS vector for silencing. Synonymous substitutions were introduced into synthetic *NRC4* (*NRC4*^{syn}) without changing the protein sequence. The nucleotide and protein sequence alignments indicate the synonymous changes in the synthetic variant. (**B**) Protein accumulation of NRC4 variants in VIGS control (EV) and *NRC4*-silenced plants. N-terminal GFP-tagged NRC4 variants were transiently expressed in VIGS control and *NRC4*-silenced *N. benthamiana*. Samples were collected at 3 dpi for immunoblot analysis. (**C**) Accumulation of Rpi-blb2 in *NRC4*-silenced *N. benthamiana*. RFP:Rpi-blb2 was transiently expressed in VIGS control and *NRC4*-silenced *N. benthamiana*. Samples were collected at 3 dpi for immunoblot analysis. (**D**) Semi-quantitative RT-PCR of members in the NRC family. Leaves were collected three weeks after virus inoculation. The expression of *NRC2*, *NRC3*, *NRC4* and *NRC4L-4611* (NbS00004611g0006) were analyzed. Elongation factor -1α (EF1α) was used as an internal control.

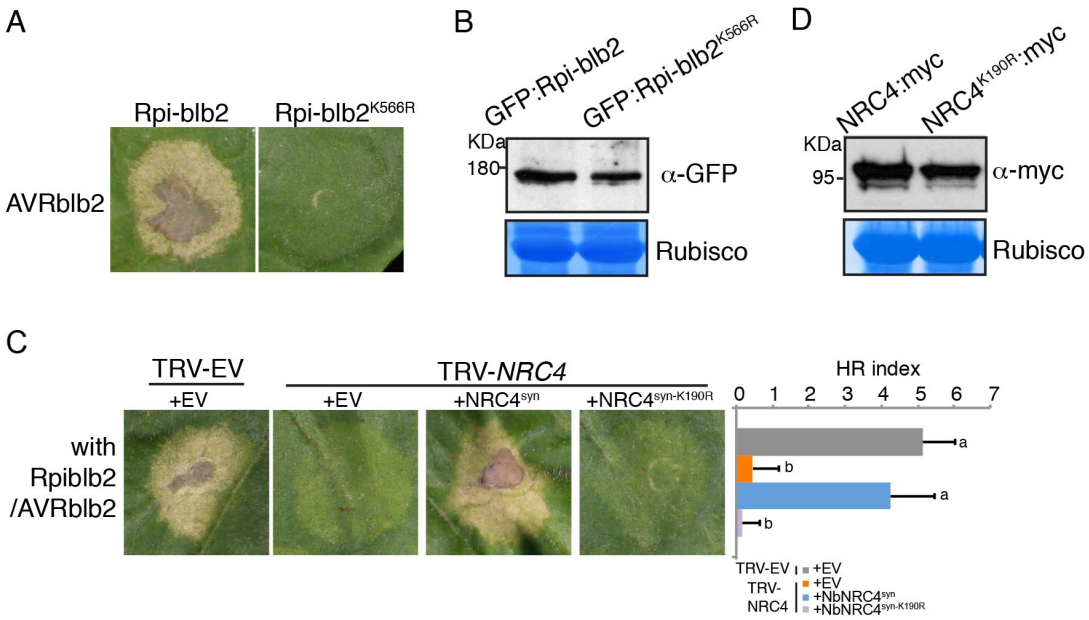

Fig. S2. Activities of both Rpi-blb2 and NRC4 are p-loop dependent

(A) P-loop is essential for the activity of Rpi-blb2. Wild type Rpi-blb2 and the p-loop mutant (K566R) were co-expressed with AVRblb2 in *N. benthamiana*. Images were taken 7 days after agroinfiltration. (**B**) Accumulation of Rpi-blb2 and Rpi-blb2 p-loop mutant. GFP:Rpi-blb2 variants were expressed in *N. benthamiana* by agroinfiltration. Samples were collected at 3 dpi for immunoblot analysis. (**C**) P-loop is essential for activity of NRC4. A lysine to arginine mutation was introduced into the p-loop of synthetic *NRC4*, and then the activity was examined by co-expression with Rpi-blb2 and AVRblb2 in *NRC4*-silenced plants. Hypersensitive cell death (HR) was scored at 7 days after agroinfiltration. Bars represent mean + SD of 24 infiltration sites. Statistical differences among the samples were analyzed with ANOVA and Tukey's HSD test (p-value < 0.001). (**D**) Accumulation of NRC4 and NRC4 p-loop mutant. NRC4:myc variants were expressed in *N. benthamiana* by agroinfiltration. Samples were collected at 3 dpi for immunoblot analysis.

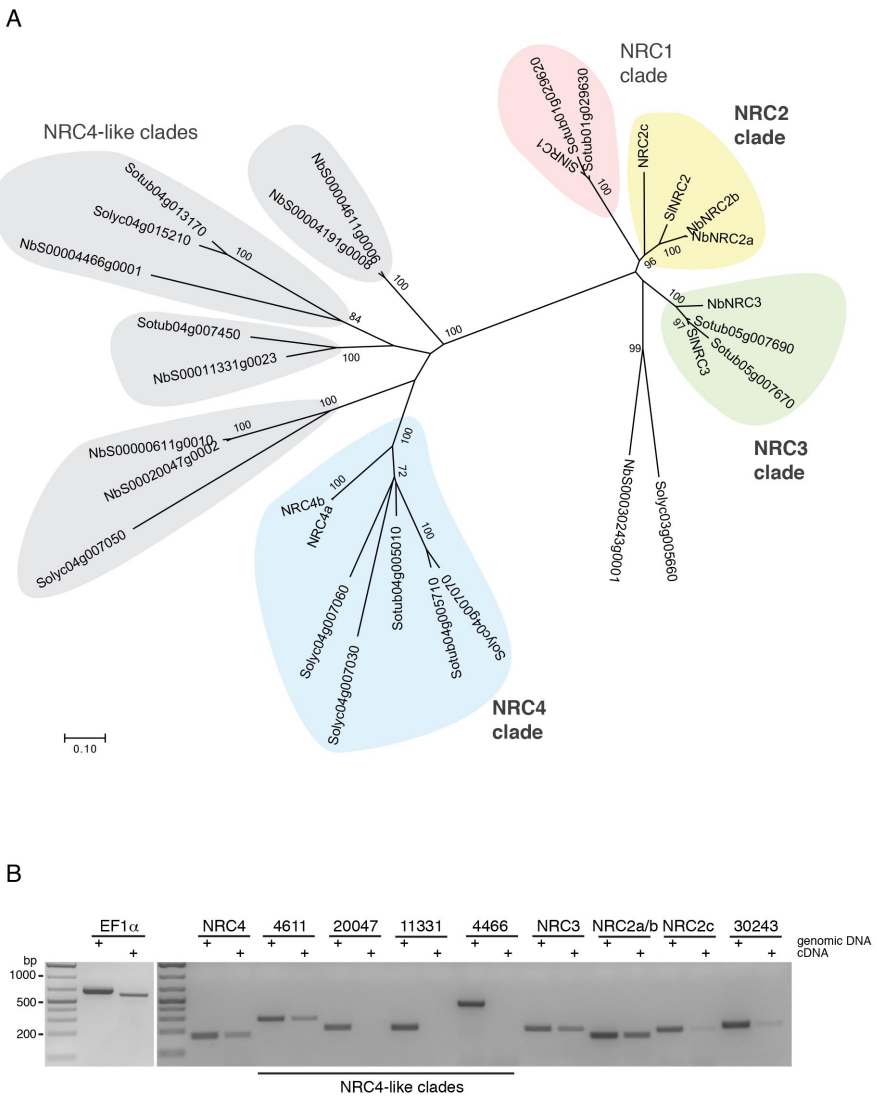

Fig. S3. Phylogeny and PCR analysis of NRC family members

(**A**) Maximum-likelihood phylogenetic tree of NRC family members. Protein sequences of NRC family members identified from *N. benthamiana* (NbS-), tomato (Solyc-), and potato (Sotub-) were aligned by using Clustal Omega, and then the NB-ARC domains were used for the further analysis. Phylogenetic tree was constructed in MEGA7 with Jones-Taylor-Thornton (JTT) substitution model and 1000 bootstrap iterations. Branches with bootstrap support higher than 70 are indicated. NRC1, NRC2, NRC3, NRC4 and NRC4-like clades were marked with red, green, yellow, blue and grey, respectively. The scale bar indicates the evolutionary distance in amino acid substitution per site. (**B**) PCR and RT-PCR analysis of NRC family members. Primer pairs were designed based on cDNA sequences identified from *N. benthamiana* genome database. PCR with *N. benthamiana* genomic DNA (gDNA) was used to confirm the amplification with the primers. RT-PCR was used for checking the expression of the corresponding genes. Genes in the NRC4-like clades are labeled with the digital numbers from the accession numbers in (**A**).

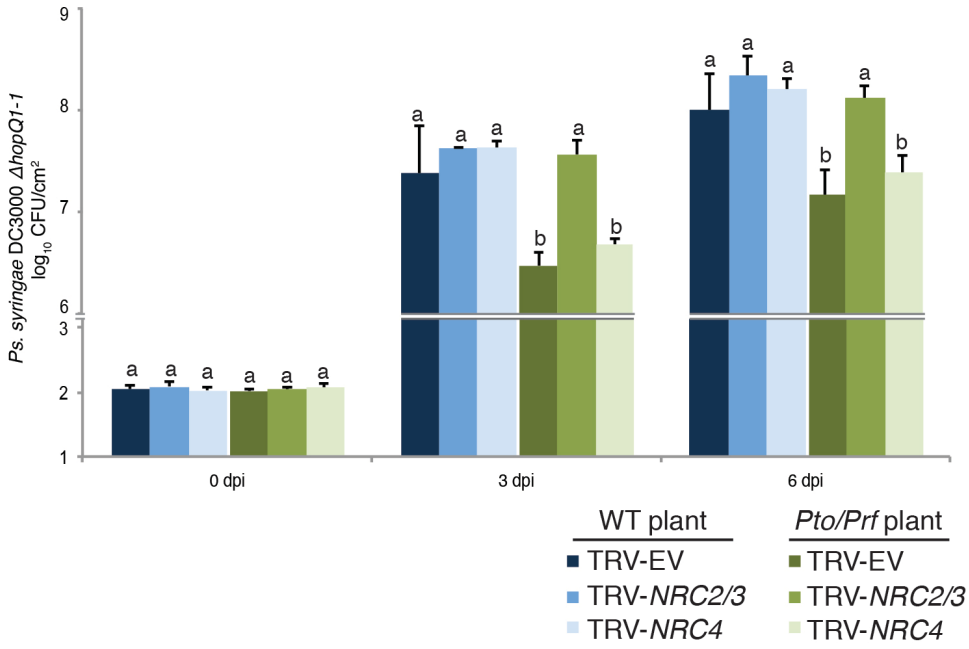

Fig. S4. *NRC4* is not required for Prf-mediated resistance

Bacterial growth assay of *Pseudomonas syringae* pv. *tomato* DC3000 *ΔhopQ1-1* in *NRC*-silenced *Pto/Prf* transgenic *N. benthamiana*. *NRC2/3* or *NRC4* were silenced in wild type or *Pto/Prf* transgenic *N. benthamiana* by VIGS. *Ps. syringae* pv. *tomato* DC3000 *ΔhopQ1-1* was infiltrated into *N. benthamiana* by using a needleless syringe and samples were collected at 0, 3, and 6 days post inoculation (dpi). The bars represent mean + standard deviation (SD) of population from four technical replicates in one representative biological replicate. The different letters at the top of the columns indicate statistically significant differences based on ANOVA and Tukey's HSD test (p-value < 0.05). Experiments were performed three times with similar results.

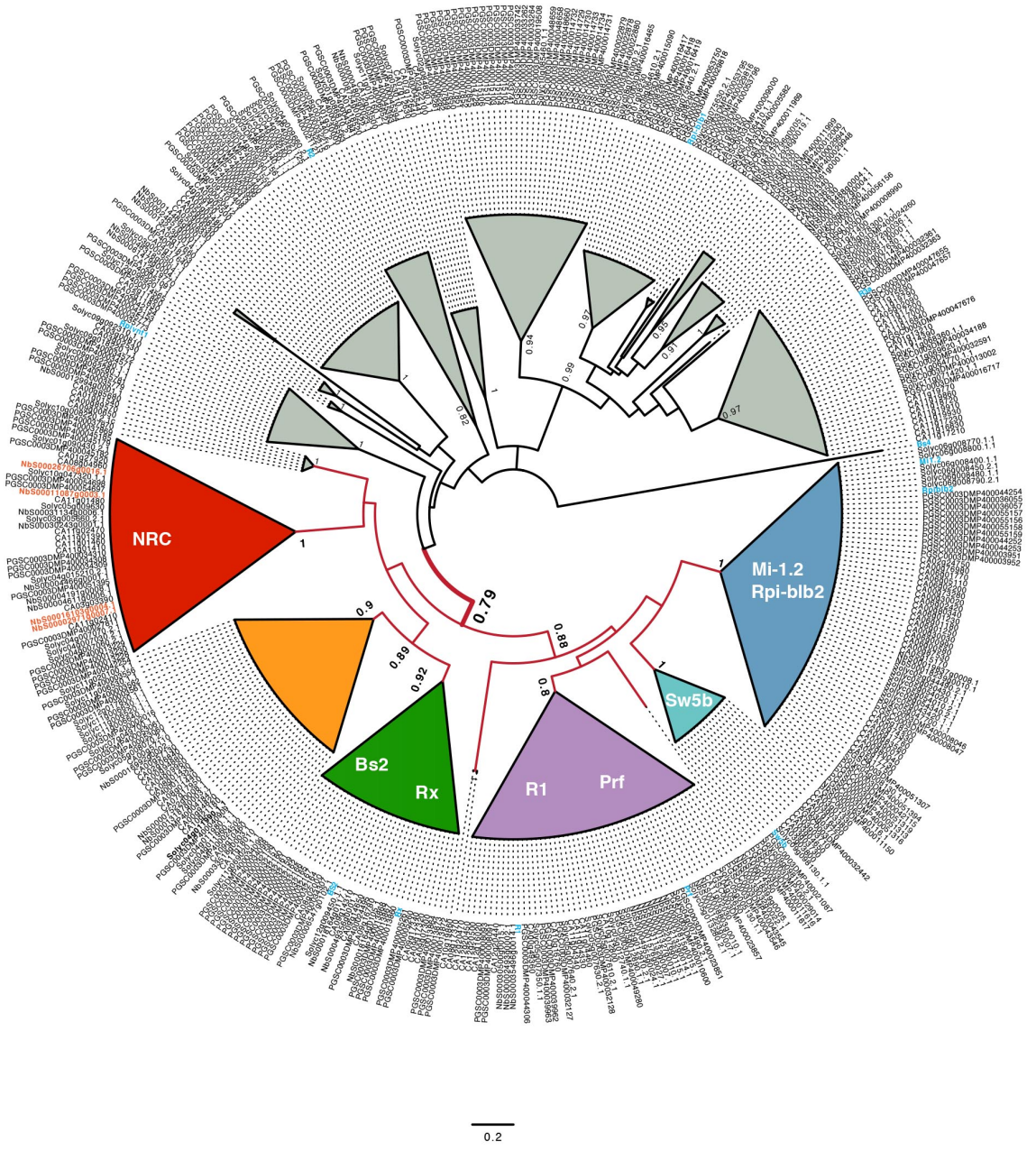

Fig. S5. Phylogenetic analysis of solanaceous CNL proteins

CNL proteins identified by NLR-parser from *N. benthamiana* (NbS-), tomato (Solyc-), potato (PGSC-) and pepper (CA-) were analyzed by MEGA7 to generate maximum-likelihood phylogenetic tree. Only the NB-ARC domains of the sequences were used in the analysis. Sequences of several solanaceous CNL-type resistance proteins (marked in blue) were included as reference for different clades. Accession numbers of *N. benthamiana* NRC homologs are marked in orange. The scale bar indicates the evolutionary distance in amino acid substitution per site. Branches with bootstrap support higher than 0.7 are indicated.

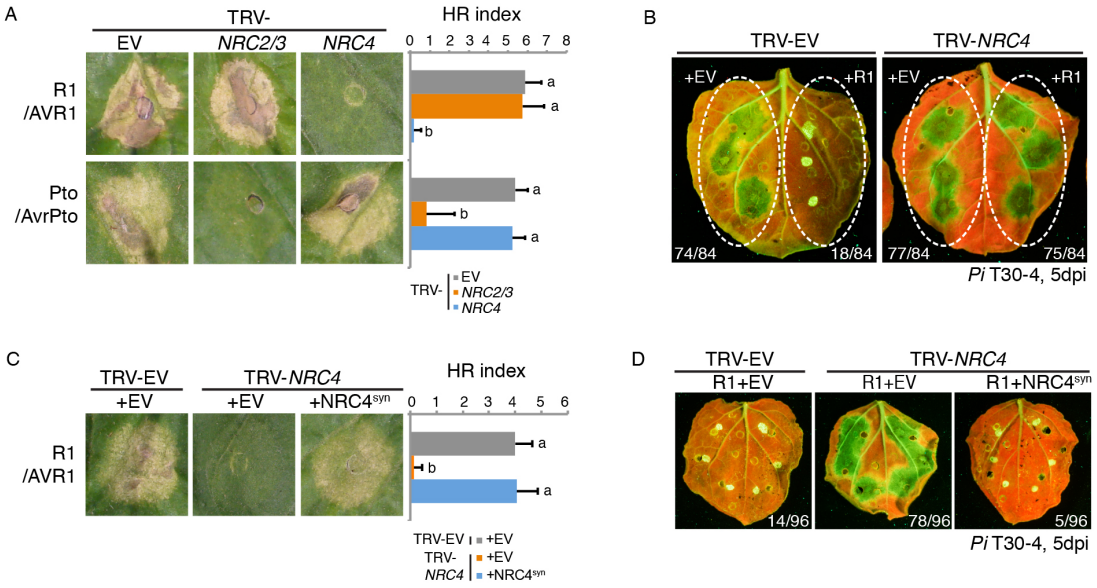

Fig. S6. Silencing of *NRC4* abolished R1-mediated immunity

(**A**) Silencing of *NRC4* abolished R1-mediated cell death. R1/AVR1 or Pto/AvrPto were expressed in *NRC2/3* or *NRC4*-silenced plants. Hypersensitive cell death (HR) was scored at 7 days after agroinfiltration. Bars represent mean + SD from 24 infiltration sites. Statistical differences among the samples were analyzed with ANOVA and Tukey's HSD test (p-value < 0.001). (**B**) Silencing of *NRC4* abolished R1-mediated resistance. R1 or empty vector control was transiently expressed in *NRC4*-silenced or control *N. benthamiana* one day before pathogen inoculation. The leaves were inoculated with droplets of 10μL zoospore suspension (200 zoospores/μL) from *P. infestans* T30-4. Experiments were repeated 4 times with 21 inoculation sites each time. The numbers on the right bottom are the sum of spreading lesion/total inoculation sites from the four replicates. Images were taken under UV light at 5 days post inoculation (dpi). (**C**) Expression of synthetic *NRC4* rescued R1-mediated cell death in *NRC4*-silenced plants. R1/AVR1 were co-expressed with synthetic NRC4 or empty vector control in *NRC4*-silenced or control plants through agroinfiltration. Hypersensitive response (HR) was scored at 7 days after agroinfiltration. Bars represent mean + SD of 24 infiltration sites. Statistical differences among the samples were analyzed with ANOVA and Tukey's HSD test (p-value < 0.001). (**D**) Expression of synthetic *NRC4* rescued R1-mediated resistance in *NRC4*-silenced plants. Synthetic *NRC4* or empty vector were co-expressed with R1 into *NRC4*-silenced or control plants one day before *P. infestans* inoculation. Experiments were repeated 4 times with 24 inoculation sites each time. The numbers on the right bottom are the sum of spreading lesion/total inoculation sites from the four biological replicates. Images were taken under UV light at 5 days post inoculation (dpi).

A

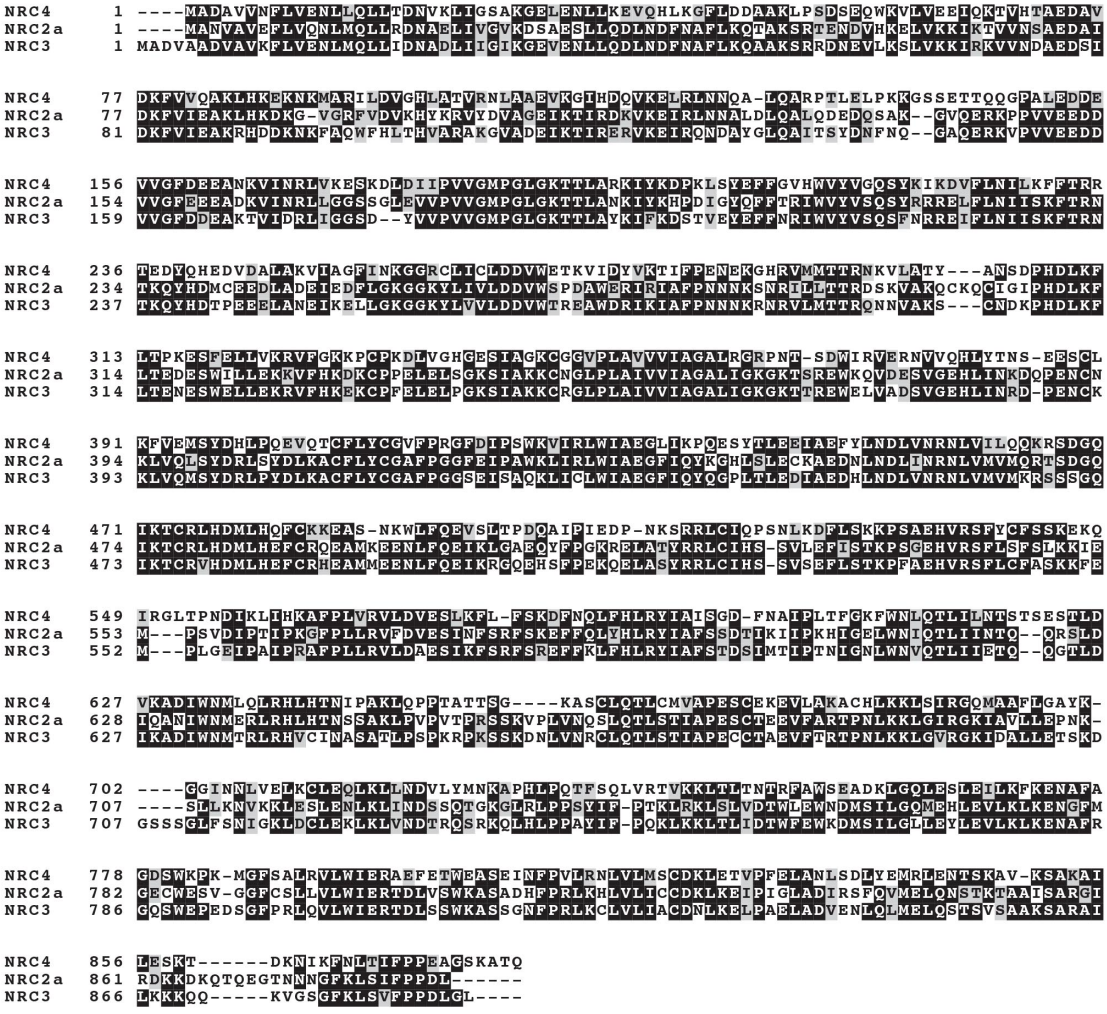

B

Sequence identity/similarity

	NRC2a	NRC3
NRC3	69/80	
NRC4	48/66	49/66

Fig. S7. Sequence alignment and pairwise comparisons of NRC2/3/4

(A) Protein sequences of NRC2/3/4 were aligned with Clustal Omega and analyzed by BoxShade. Identical amino acids are highlighted in black and conserved amino acids are highlighted in grey. (B) Pairwise comparisons of identity/similarity of NRC2/3/4 protein sequences. Pairwise sequence comparisons were performed by aligning two sequences using BLASTP on NCBI website.

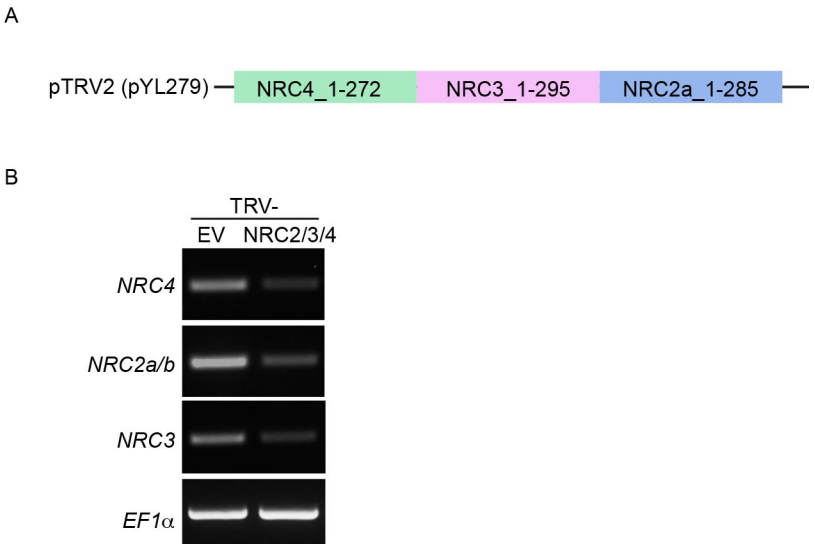

Fig. S8. *NRC2/3/4* triple silencing in *N. benthamiana*

(**A**) Schematic representation of design for *NRC2/3/4* triple silencing. Fragments from *NRC2/3/4* as indicated were combined together as one fragment and then cloned into TRV2 vector for silencing. (**B**) Semi-quantitative RT-PCR of *NRC2/3/4* triple silencing. Leaf samples were collected three weeks after virus inoculation. The expression of *NRC2*, *NRC3*, and *NRC4* were analyzed. Elongation factor 1α (EF1α) was used as an internal control.

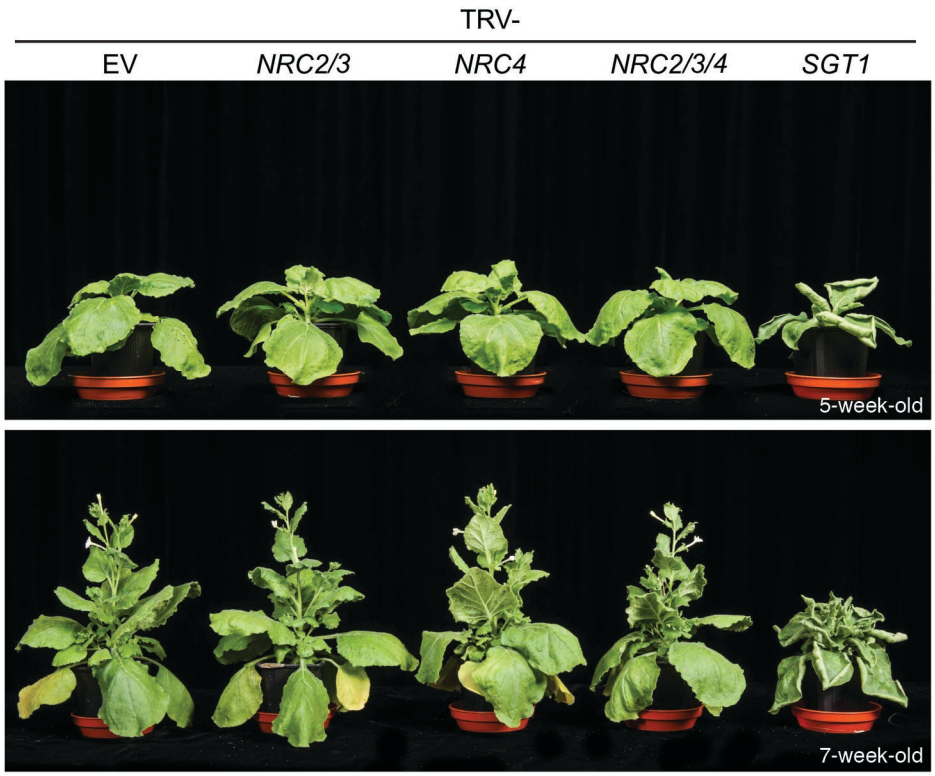

Fig. S9. Silencing of *NRC* homologs does not affect growth of *N. benthamiana*

NRC homologs or *SGT1* were silenced in *N. benthamiana*, and the plants were left in the greenhouse without any further treatment. Photos were taken at 3 weeks and 5 weeks after TRV inoculation, corresponding to 5 weeks and 7 weeks after sowing.

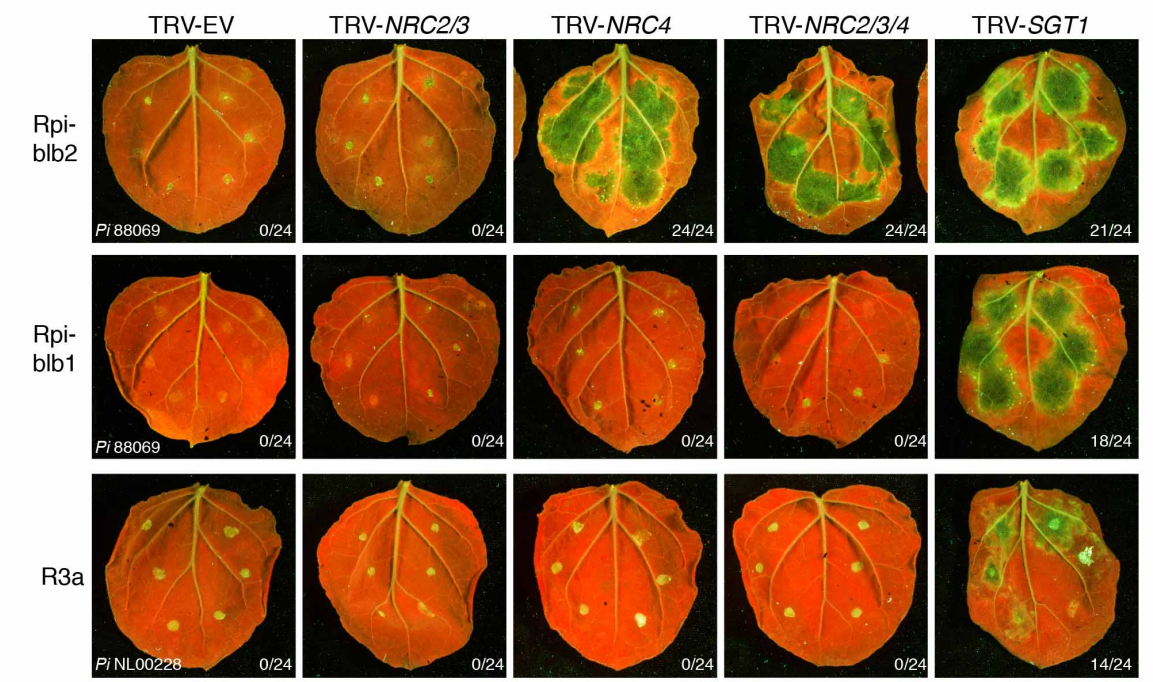

Fig. S10. Silencing of *NRC2/3/4* does not affect resistance mediated by R3a and Rpi-blb1

NRC2/3/4 were silenced individually or in combinations in *Rpi-blb2*, *R3a*, and *Rpi-blb1* transgenic plants. *SGT1* silencing was used as a control. *P. infestans* 88069 or NL00228 were inoculated on the leaves, and photos were taken under UV light at 4 days post inoculation (*Pi* 88069) or 5 days post inoculation (*Pi* NL00228). The numbers on the right bottom are the sum of spreading lesion/ total inoculation sites from one representative biological replicate.

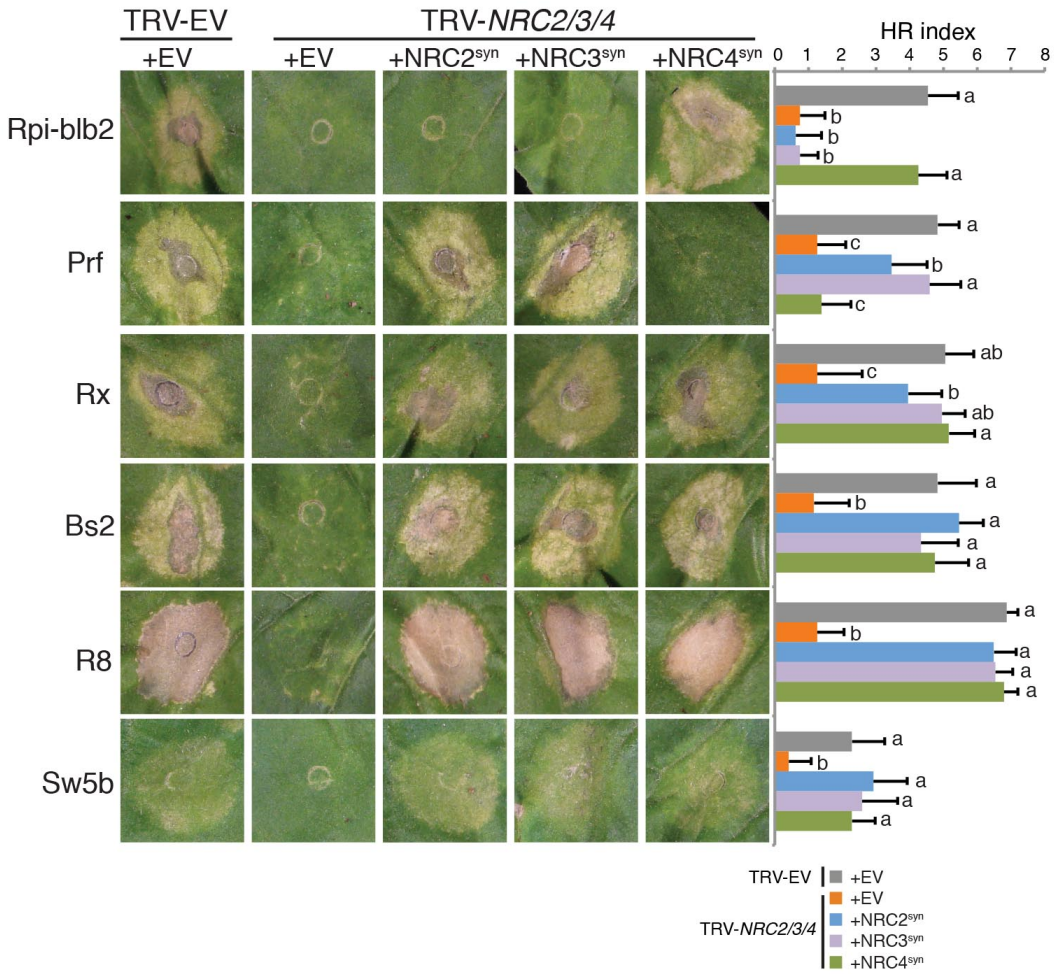

Fig. S11. *NRC2/3/4* display specificity and redundancy to different sensor NLRs from the NRC-superclade

Rpi-blb2, Pto (Prf), Rx, Bs2, R8, and Sw5b were co-expressed with the corresponding AVR proteins and synthetic *NRC2*, *NRC3* or *NRC4* in *NRC2/3/4*-silenced *N. benthamiana*. Hypersensitive cell death (HR) was scored at 7 days after agroinfiltration. Bars represent mean + SD of 24 infiltration sites. Statistical differences among the samples were analyzed with ANOVA and Tukey's HSD test (p-value < 0.001).

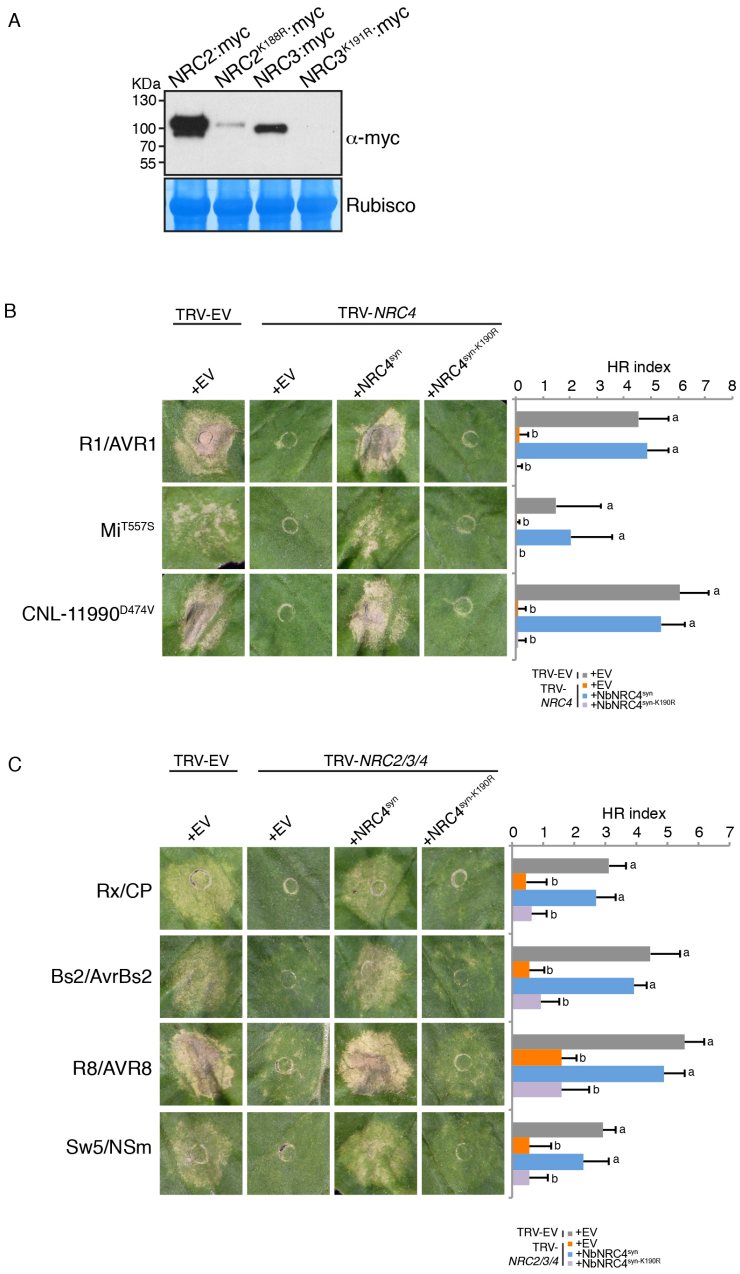

Fig. S12. P-loop is essential for NRC4 function in all the tested helper-sensor combinations

(**A**) Accumulation of wild type and p-loop mutants of NRC2, NRC3. NRC2 and NRC3 variants were expressed in *N. benthamiana* by agroinfiltration. Samples were collected at 3 dpi for immunoblot analysis. (B) and (C) P-loop of is required for activity of NRC4 in all the tested helper-sensor NLR combinations. Wild type NRC4 and the p-loop mutant (K190R) were co-expressed with different NLRs with corresponding AVR or autoactive NLRs in *NRC4*-silenced (B) or *NRC2/3/4*-silenced (C) *N. benthamiana* leaves. Hypersensitive cell death (HR) was scored at 6 days after agroinfiltration. Bars represent mean + SD of 24 infiltration sites. Statistical differences among the samples were analyzed with ANOVA and Tukey's HSD test (p-value < 0.001).

Fig. S13. Systemic spread of trailing necrosis induced by PVX in *NRC2/3/4*-silenced *Rx* plant

Control (EV) and *NRC2/3/4*-silenced *Rx* plants in Fig. 3 were left in growth chamber until 5 weeks post PVX inoculation (wpi). The susceptible wild type (WT) plant and resistant Rx plant showed normal senescence and/or viral symptoms, whereas the *NRC2/3/4*- and *SGT1*-silenced plants displayed trailing necrotic lesions throughout the whole plant.

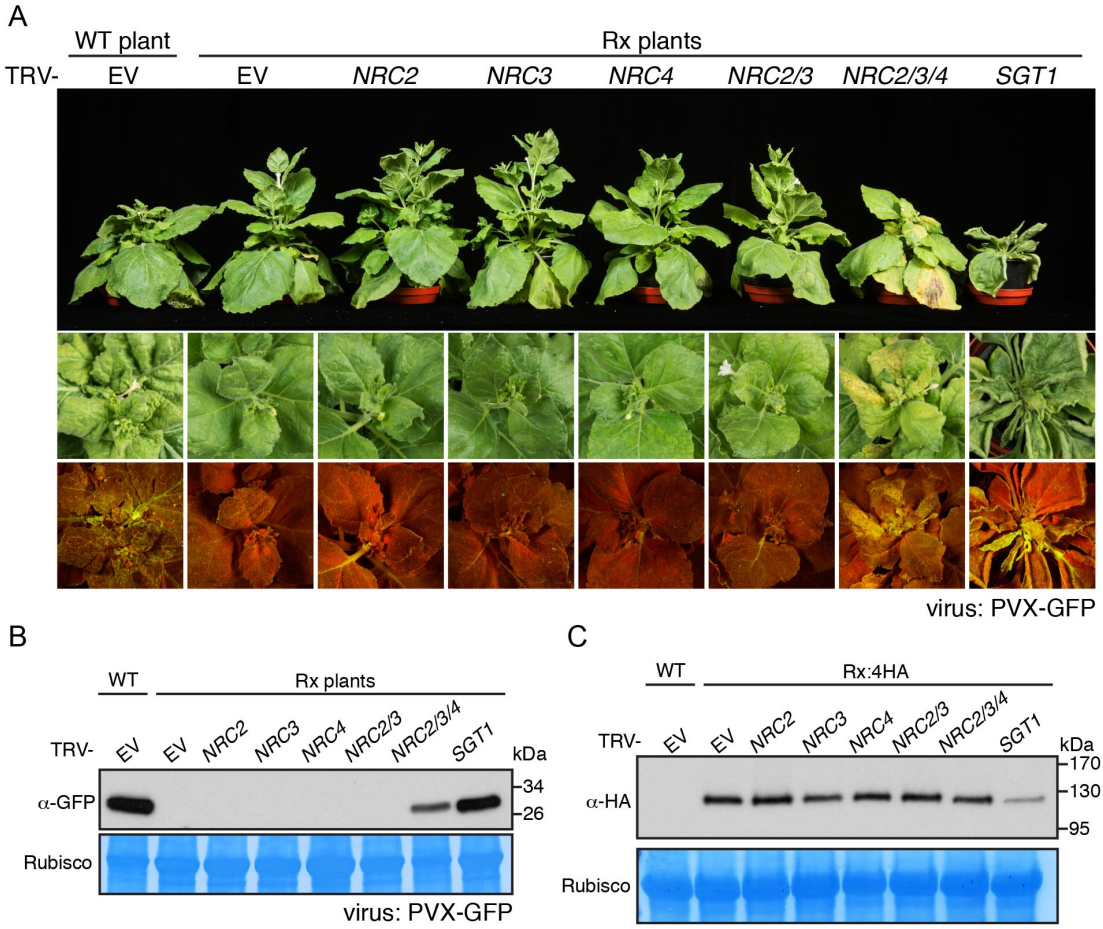

Fig. S14. *NRC2/3/4* triple silencing compromised Rx-mediated extreme resistance to PVX

(**A**) Triple silencing of *NRC2/3/4* compromised Rx-mediated resistance to PVX-GFP. Experiments were performed in the same way as Fig. 3, but inoculated with PVX-GFP (pGR106-GFP). The pictures were taken under daylight and UV light at 2 weeks after PVX inoculation. (**B**) Immunoblot analysis of GFP accumulation with upper leaves collected from (**A**). (**C**) Silencing of *NRC2/3/4* did not affect accumulation of Rx. *NRC2, NRC3* or *NRC4* were silenced individually or in combinations in Rx transgenic plants (Rx:4HA). *SGT1* silencing, which compromises Rx protein accumulation and Rx-mediated resistance (29), was used as a control for the experiments. Leaf samples were collected three weeks after TRV inoculation for immunoblot analysis.

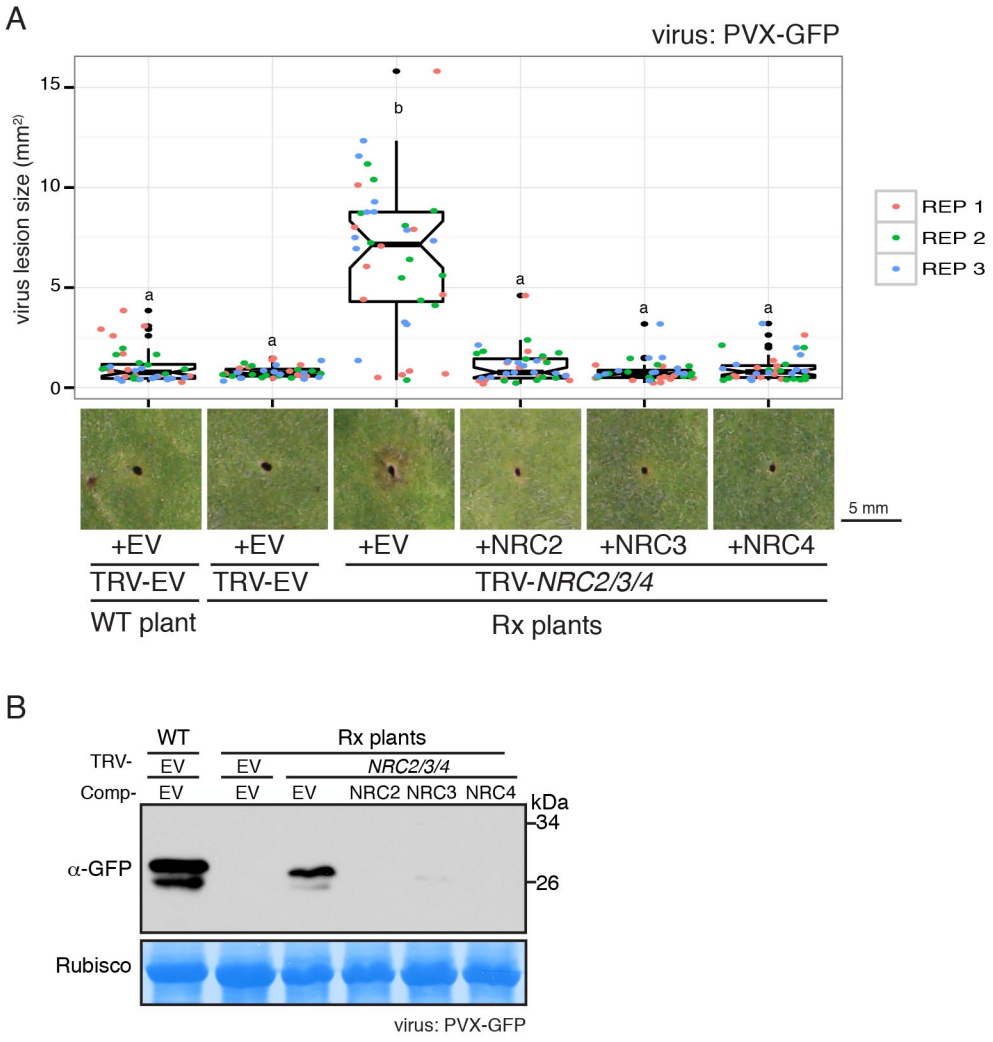

Fig. S15. Validation of *NRC2/3/4* redundancy in Rx-mediated resistance

(**A**) Expression of synthetic *NRC2*, *NRC3* or *NRC4* rescued Rx-mediated resistance in *NRC2/3/4*-silenced plants. *NRC2/3/4* were silenced together in *Rx* transgenic *N. benthamiana* and then synthetic *NRC2*, *NRC3*, or *NRC4* were expressed on the leaves one day before PVX inoculation. PVX-GFP was inoculated on the leaves by using toothpick inoculation method. Pictures were taken at 10 days after PVX inoculation and the size of necrotic lesions were measured by using Image J. Data acquired from different biological replicates (REP) were presented with different colors. Statistical differences among the samples were analyzed with ANOVA and Tukey's HSD test (p-value < 0.01). (**B**) Immunoblot analysis of GFP accumulation in leaf discs collected from (**A**). "Comp-", complementation.

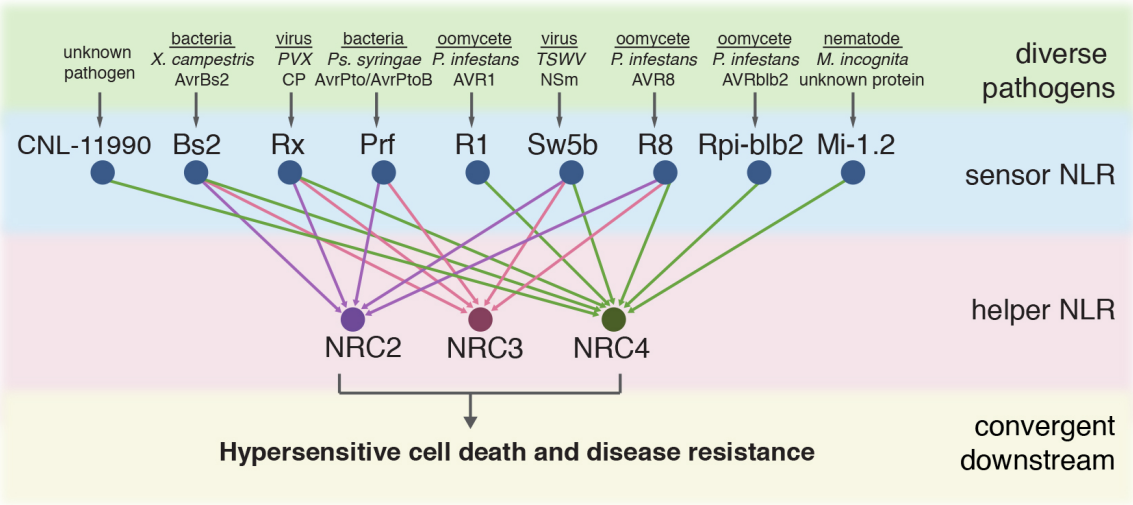

Fig. S16. A NRC-dependent NLR immune signaling network provides resistance to diverse pathogens

A schematic view of the NRC-dependent NLR immune signaling network based on the analysis in *N. benthamiana*. Several NLRs that confer resistance to diverse pathogens, including virus, bacteria, oomycete, nematodes and insects converge on the three NRC proteins. These three NRC proteins are functionally redundant but also display specificity toward some of the sensor NLRs. Similar to other plant NLRs, the downstream signaling remains largely unknown.

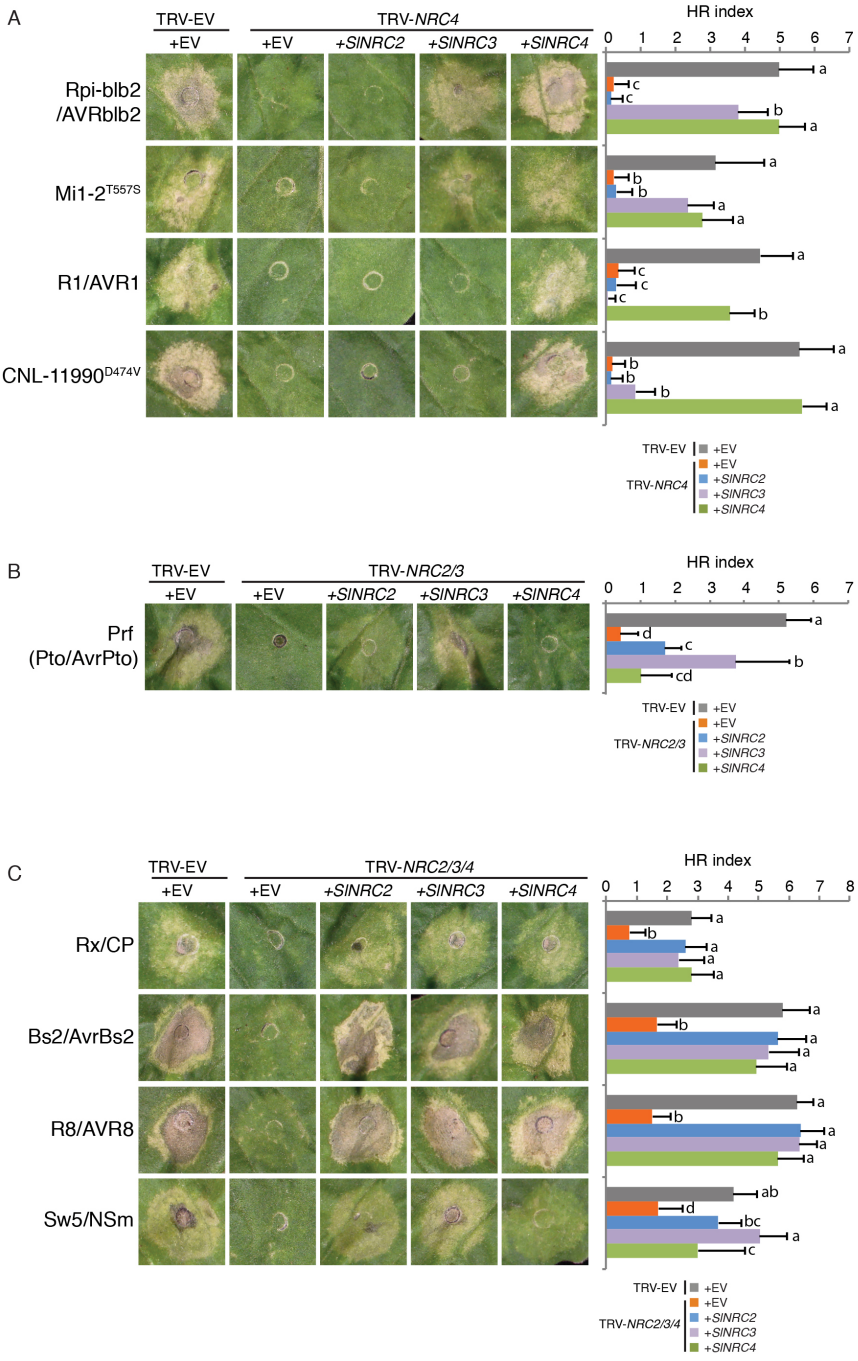

Fig. S17. Expression of tomato NRC homologs rescue NRC-dependent cell death in *N. benthamiana*

Tomato NRC homologs (*SlNRC2*, *SlNRC3*, *SlNRC4*) were co-expressed with different NLRs with corresponding AVR or autoactive NLRs in *NRC4*-silenced (A) or *NRC2/3/4*-silenced (B) *N. benthamiana* leaves. Hypersensitive cell death (HR) was scored at 6 days after agroinfiltration. Bars represent mean + SD of 24 infiltration sites. Statistical differences among the samples were analyzed with ANOVA and Tukey's HSD test (p-value < 0.001).

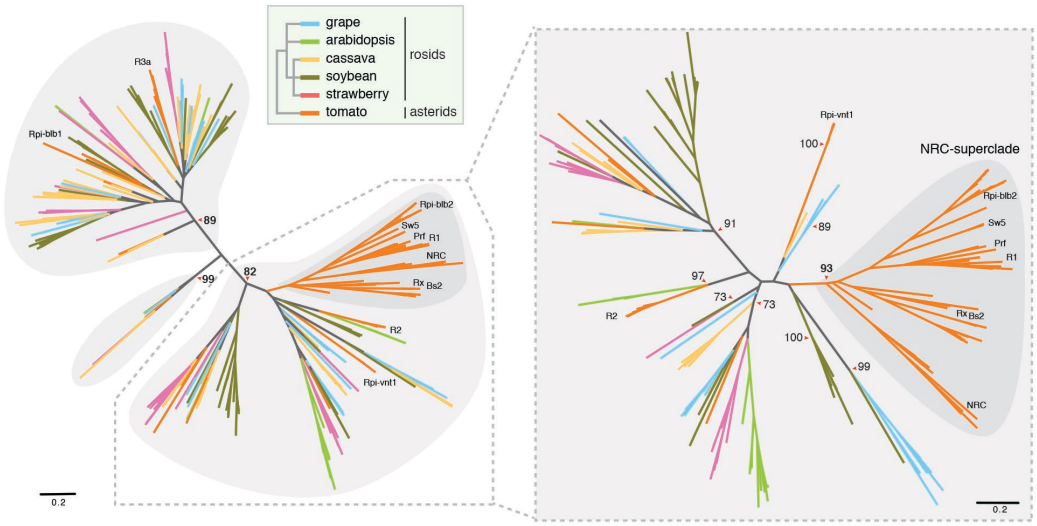

Fig. S18. The NRC-superclade emerged after the divergence of rosids and asterids

Phylogeny of CNL identified from rosids (grape, arabidopsis, cassava, soybean, and strawberry) and asterids (tomato). CNL identified from indicated species were aligned by using MAFFT and analyzed in MEGA7 to generate maximum-likelihood phylogenetic tree. Only the NB-ARC domains of the sequences were used in the analysis. Sequences identified from different species were presented with different colors as indicated. The bootstrap supports of the major nodes are indicated. The phylogenetic trees at the right panel, which include only the sequences from the indicated lineages in the left panel, indicated that NRC helper/sensor sequences form a well-supported superclade that existed in asterids but not rosids. The scale bars indicate the evolutionary distance in amino acid substitution per site. Details of the full phylogenetic tree can be found in Fig. S19-20.

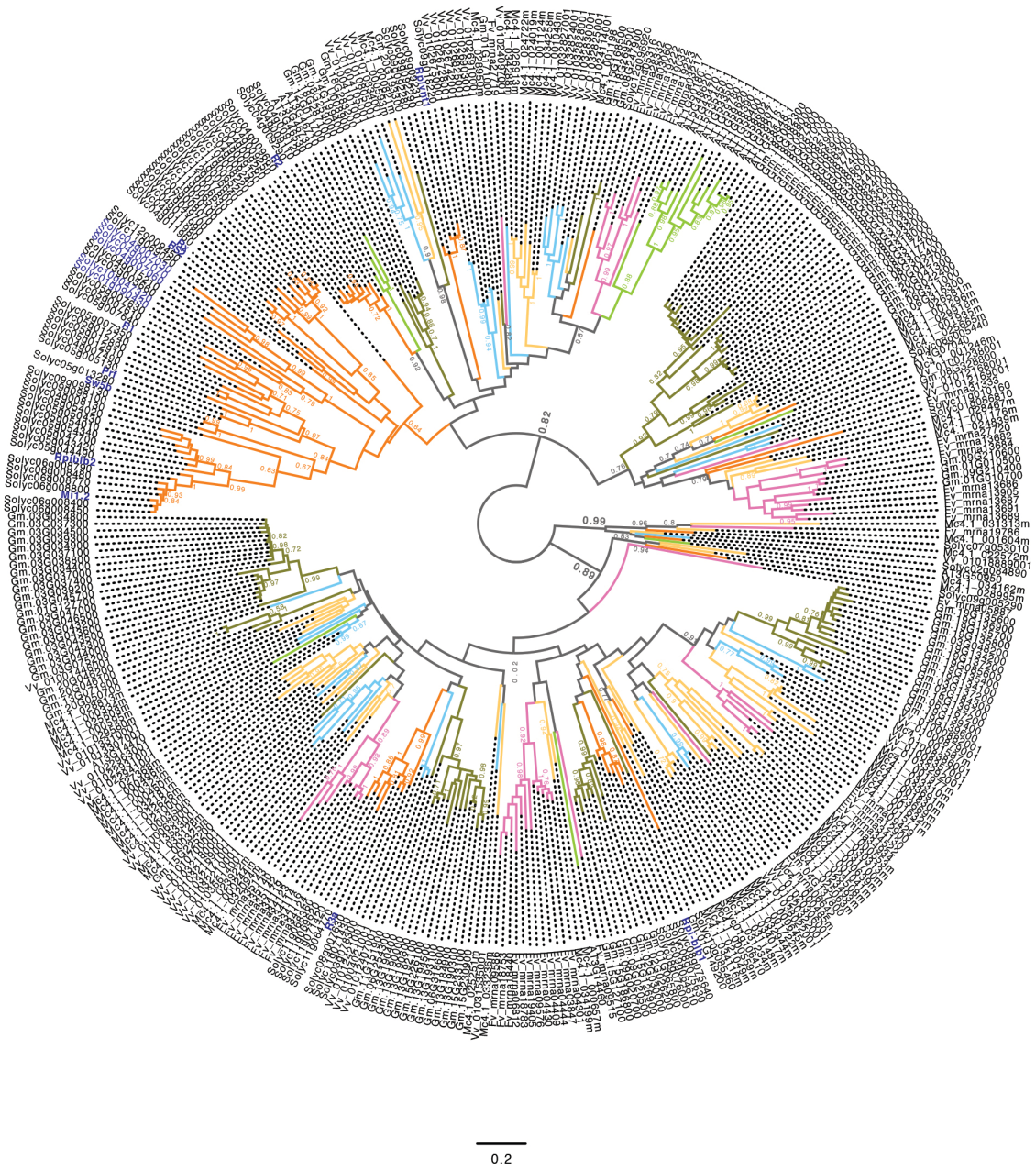

Fig. S19. Phylogenetic tree of CNL identified from rosids and asterids I

Polar tree layout of phylogeny presented in the left panel of Fig. S18. Branches with bootstrap support higher than 0.7 are indicated.

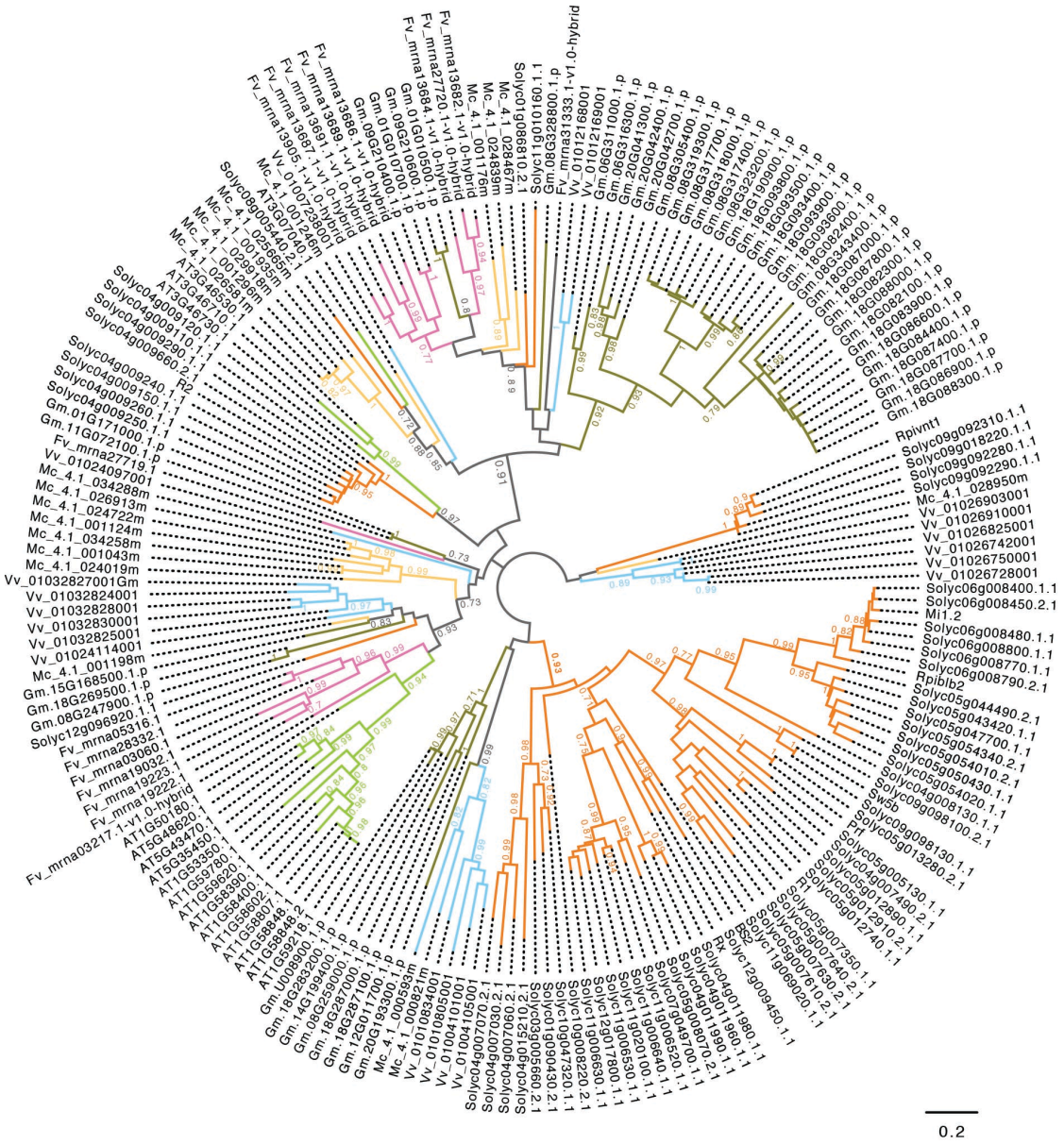

Fig. S20. Phylogenetic tree of CNL identified from rosids and asterids II

Polar tree layout of phylogeny presented in the right panel of Fig. S18. Branches with bootstrap support higher than 0.7 are indicated.

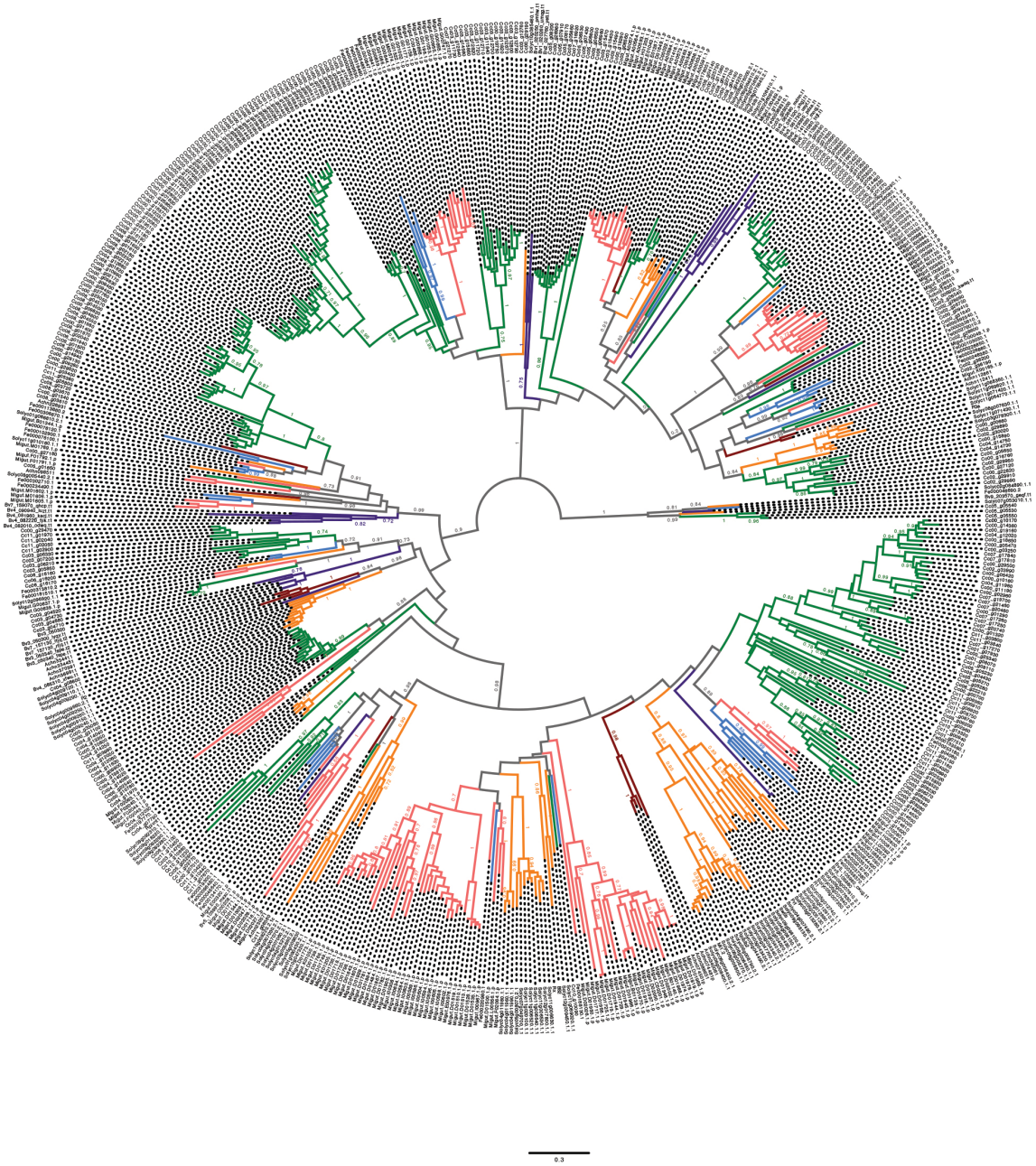

Fig. S21. Phylogenetic tree of CNL identified from asterids and caryophyllales I

Polar tree layout of phylogeny presented in the left panel of Fig. 4A. Branches with bootstrap support higher than 0.7 are indicated.

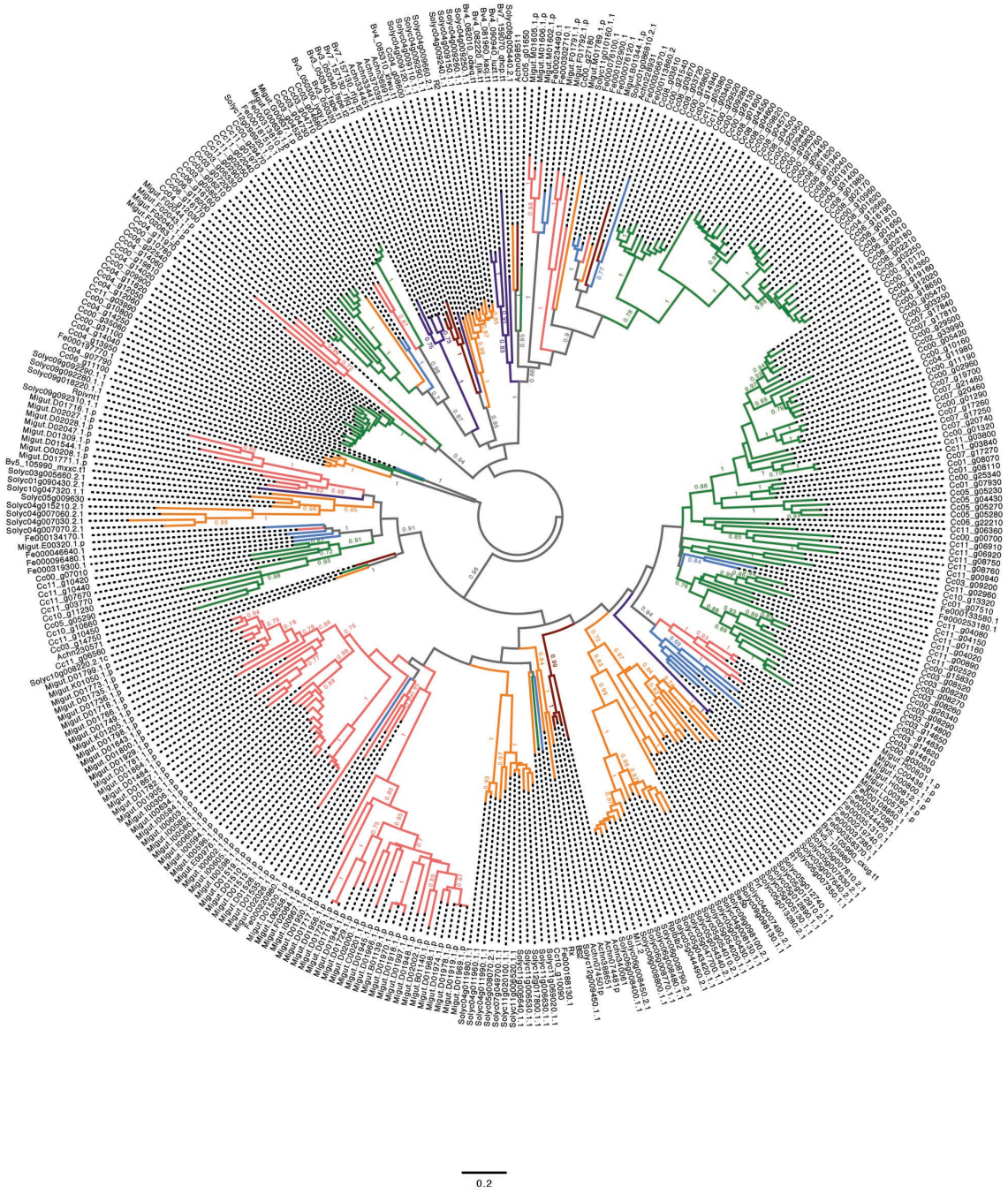

Fig. S22. Phylogenetic tree of CNL identified from asterids and caryophyllales II

Polar tree layout of phylogeny presented in the right panel of Fig. 4A. Branches with bootstrap support higher than 0.7 are indicated.

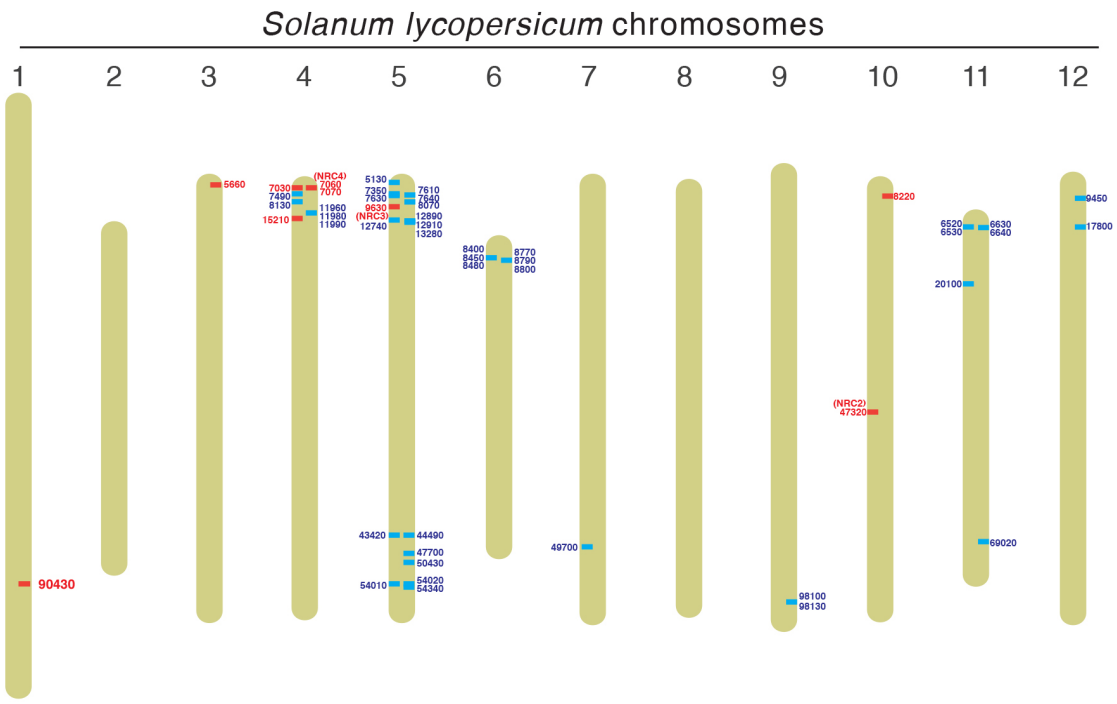

Fig. S23. Chromosomal locations of NRC-H/S homologs in tomato

Locations of tomato NRC-H/S homologs on the chromosomal map modified from Andolfo et al. (2014). NRC-H homologs are marked in red, and NRC-S homologs are marked in blue.

Table S1. List of characterized CNLs from solanaceous plants

Gene name	Origin species	Pathogen and protein recognized	Clade in Andolfo et. al. (2014)	Clade in Seo et. al. (2016)	In NRC-superclade (Yes/No)	NRC-dependent (Yes/No)	Reference
Rpi-blb2	*Solanum bulbocastanum*	*P. infestans*, AVRblb2	CNL-1	CNL-G1	Y	Y	(30)
Mi-1.2	*Solanum peruvianum*	*Meloidogyne spp.* *Macrosiphum euphorbiae* *Bemisia tabaci*	CNL-1	CNL-G1	Y	Y	(31)
Pvr9	*Capsicum annuum*	*Pepper mottle virus, NIb*	CNL-1	CNL-G1	Y	n.d.	(32)
Hero	*Solanum pimpinellifolium*	*Globodera rostochiensis* *Globodera pallida*	CNL-9	CNL-G1	Y	n.d.	(33)
Sw-5b	*Solanum peruvianum*	*Tomato spotted wilt virus*, NSm	CNL-10	CNL-G6	Y	Y	(15)
R8	*Solanum demissum*	*P. infestans*, AVR8	CNL-10	CNL-G6	Y	Y	(34)
R1	*Solanum demissum*	*P. infestans*, AVR1	CNL-11	CNL-G3	Y	Y	(35)
Prf	*Solanum pimpinellifolium*	*Ps. syringae*, AvrPto/AvrPtoB	CNL-11	CNL-G3	Y	Y	(36)
Rx1	*Solanum andigena*	*Potato virus X*, CP	CNL-2	CNL-G12	Y	Y	(37)
Rx2	*Solanum acaule*	*Potato virus X*, CP	CNL-2	CNL-G12	Y	n.d.	(38)
Gpa2	*Solanum pimpinellifolium*	*Globodera pallida*, RBP-1	CNL-2	CNL-G12	Y	n.d.	(39)
Bs2	*Capsicum chacoense*	*Xanthomonas campestris*, AvrBs2	CNL-12	CNL-G2	Y	Y	(40)
Rpi-amr3	*Solanum americanum*	*P. infestans*	CNL-13	CNL-G9	Y	n.d.	(41)
Rpi-vnt1	*Solanum venturii*	*P. infestans*, Avrvnt1	CNL-4	CNL-G11	N	N	(42, 43)
Tm2	*Solanum peruvianum*	*Tomato mosaic virus,* MP *Tobacco mosaic virus,* MP	CNL-4	CNL-G11	N	n.d.	(44)
Rpi-mcq1	*Solanum mochiquense*	*P. infestans*	CNL-4	CNL-G11	N	n.d.	(45)
R9a	*Solanum demissum*	*P. infestans*	CNL-4	CNL-G11	N	n.d.	(46)
Ph3	*Solanum pimpinellifolium*	*P. infestans*	CNL-4	CNL-G11	N	n.d.	(47)
R2	*Solanum demissum*	*P. infestans*, AVR2	CNL-5	CNL-G5	N	N	(48)
Rpi-blb3	*Solanum bulbocastanum*	*P. infestans*	CNL-5	CNL-G5	N	n.d.	(49)
Rpi-chc1	*Solanum chacoense*	*P. infestans*	CNL-7/16	CNL-G13	N	n.d.	(50)
Rpi-blb1	*Solanum bulbocastanum*	*P. infestans*, AVRblb1	CNL-6	CNL-G7	N	N	(51)
I2	*Solanum pimpinellifolium*	*Fusarium oxysporum*, AVR2	CNL-8	CNL-G4	N	n.d.	(52)
R3a	*Solanum demissum*	*P. infestans*, AVR3a	CNL-8	CNL-G4	N	N	(53)
R3b	*Solanum demissum*	*P. infestans*, AVR3b	CNL-8	CNL-G4	N	n.d.	(54)
L^1-L^4	*Capsicum* spp.	*Tobamovirus* spp. CP	CNL-8	CNL-G4	N	n.d.	(55)

n.d., not determined experimentally.

Table S2. List of transgenic *N. benthamiana* lines used in this study

NLR expressed	Pathogen recognized	Effector /avirulence factor	Reference
Prf:5myc **(with *Pto*)**	*Pseudomonas syringae* pv. *tomato DC3000*	AvrPto, AvrPtoB	R411B (13)
Rpi-blb2	*Phytophthora infestans*	AVRblb2	(56)
Rx:4HA	*Potato virus X*	Coat protein	(57)
R3a	*Phytophthora infestans*	AVR3a	(58)
Rpi-blb1	*Phytophthora infestans*	AVRblb1	(59)

Table S3. List of primers used for *NRC4* and *Rpi-blb2* cloning

Primer name	Sequence (5'-3')	Usage in this study	Reference
NRC4_CACC_F	*CACCATGGCAGATGCAGTAGTGAATTTTCT*	Gateway cloning of NRC4	This study
NRC4_R	*TCAGAAAACATGAGTAGCACCATATCCATG*	Gateway cloning of NRC4 (3'UTR)	This study
GG_NRC4_F	*AATTGGTCTCTAATGGCAGATGCAGTAGTGAATTTTC TGGTG*	NRC4 cloning GG	This study
GG_NRC4 _R	*ATTGGTCTCGAAGCTTACTGTGTGGCCTTGGATCCA GCTTC*	NRC4 cloning GG	This study
GG_NRC4_ns_R	*ATTGGTCTCTCGAATACTGTGTGGCCTTGGATCCAG CTTCA*	NRC4 cloning GG C-tag	This study
Rpiblb2_K566R_R	*/5-PHOS/ TCGACCTAAACCCGGCATACCAATGATCGA*	Rpi-blb2 p-loop mutant	This study
Rpiblb2_K566R_F	*/5-Phos/ ACTACTTTGGCGTACAAAGTATACAATGAT*	Rpi-blb2 p-loop mutant	This study
NRC4_K190R_R	*/5-Phos/ TCTTCCAAGTCCCGGCATACCCACCACCGG*	NRC4 p-loop mutant	This study
NRC4_K190R_F	*/5-Phos/ ACCACACTAGCAAGAAAAATCTACAAGGAT*	NRC4 p-loop mutant	This study
SlNRC4A_ CACC	*CACCATGGCAGATGCAGTGGTGAATTTTC*	Gateway cloning of tomato NRC4	This study
SlNRC4A_R	*TTAATTTTCAGGTGGGTATATGCTT*	Gateway cloning of tomato NRC4	This study

Table S4. List of primers used for PCR and RT-PCR of *Nb*NRC homologs

Primer name	Sequence (5'-3')	Usage in this study	Reference
NRC4_RT_F	*AAACAAATCTGCGGGTTGAC*	PCR/RT-PCR of NRC4	This study
NRC4_RT_R	*GGATGGCATTGAAGTCACCT*	PCR/RT-PCR of NRC4	This study
NRC4L-4611_F	*AGCTGCTGATGAGGGTCTTT*	PCR/RT-PCR of NRC4-like_4611	This study
NRC4L-4611_R	*AGGCTACGTACATCAGCCAA*	PCR/RT-PCR of NRC4-like_4611	This study
NRC4L-20047_F	*AAAATGCAGCGGATTACCAC*	PCR/RT-PCR of NRC4-like_20047	This study
NRC4L-20047_R	*GGCGAAGCAATACAAGAAGC*	PCR/RT-PCR of NRC4-like_20047	This study
NRC4L-11331_F	*GTGATCGAGCGTCTTGTTGA*	PCR/RT-PCR of NRC4-like_11331	This study
NRC4L-11331_R	*CTCTTCAATGCGTTTCGTGA*	PCR/RT-PCR of NRC4-like_11331	This study
NRC4L-04466_F	*CACCATGGATCGAGCGGTGGCTATG*	PCR/RT-PCR of NRC4-like_04466	This study
NRC4L-04466_R	*TGGCGAATTTCTCGCAATTCTTTG*	PCR/RT-PCR of NRC4-like_04466	This study
NRC3_RT_F	*CCTCGAAAAGCTGAAGTTGG*	PCR/RT-PCR of NRC3	(1)
NRC3_RT_R	*TGTCCCCTAAACGCATTTTC*	PCR/RT-PCR of NRC3	(1)
NRC2a/b_RT_F	*AGTGGATGAGAGTGTGGGTG*	PCR/RT-PCR of NRC2a/b	(1)
NRC2a/b_RT_R	*AAGCAGGGATCTCAAAGCCT*	PCR/RT-PCR of NRC2a/b	(1)
NRC2c_RT_F	*TCAAAACATGCCGTGTTCAT*	PCR/RT-PCR of NRC2c	(1)
NRC2c_RT_R	*CCTGCGGGTTTTGTACTGAT*	PCR/RT-PCR of NRC2c	(1)
NRCL-30243_F	*CCAAGTGCATCAATCTGTGG*	PCR/RT-PCR of NRC-like_30243	This study
NRCL-30243_R	*ATGGCCTTTGTTCTGGAATG*	PCR/RT-PCR of NRC-like_30243	This study
NbEF1α_F	*AAGGTCCAGTATGCCTGGGTGCTTGAC*	PCR/RT-PCR of EF1α	(60)
NbEF1α_R	*AAGAATTCACAGGGACAGTTCCAATACCAC*	PCR/RT-PCR of EF1α	(60)

Table S5. List of primers used for NLR and AVR cloning

Primer name	Sequence (5'-3')	Usage in this study	Reference
R1_F_CACC	*CACCATGAATTTCAACAATGAATTGTCTGATCTG*	Cloning of R1	This study
R1_dHMA_R2	*CTATCTTATTTCTGCAAGAATATTTTTTAC*	Cloning of R1	This study
Avr1_Pentry_F	*CACCGTGTCGAAATTGCCGTCG*	Cloning of AVR1	This study
Avr1_Pentry_R	*TTAAAATGGTACCACAACATGTCCACC*	Cloning of AVR1	This study
CNL11990_GG_F	*AATTGGTCTCTAATGGCAGCTTATAGTGCTGTAATTTC*	Cloning of CNL11990	This study
CNL11990_GG_R	*AATTGGTCTCTAAGCTTAGTTCCTGTAATTATAGATGTCGAC*	Cloning of CNL11990	This study
CNL11990_D474V_GG_R	*AATTGGTCTCTAACATGTATTCCACATGCTTTTATCTC*	Mutagenesis of CNL11990	This study
CNL11990_D474V_GG_F	*AATTGGTCTCATGTTATACTGCGCGAGTTCTGTTTGATT*	Mutagenesis of CNL11990	This study

Table S6. List of NLR and corresponding AVR used in the cell death assays

Protein name	Tag	Density (OD_{600})	Reference
Rpi-blb2	N-terminal GFP	0.2	(56)
AVRblb2	N-terminal Flag	0.1	(56, 59)
Mi-1.2^{T557S}	N-terminal TAP	0.8	(61)
Sw5b	Untagged	0.6	(16)
NSm	Untagged	0.6	(17)
R8	Untagged	0.1	(34)
AVR8	Untagged	0.05	(34)
R1	Untagged	0.2	(35)
AVR1	N-terminal GFP	0.1	(62)
Pto	C-terminal GFP	0.6	(63, 64)
AvrPto	C-terminal Flag	0.1	(63, 64)
Rx	C-terminal HA	0.1	(9, 57)
CP	C-terminal csBP	0.05	(9)
Bs2	C-terminal Flag	0.2	(40)
AvrBs2	C-terminal HA	0.1	(40)
CNL-11990^{D474V}	Untagged	0.4	This study
Rpi-vnt1	Untagged	0.1	(42, 43)
AVRvnt1	Untagged	0.05	(65)
R2	Untagged	0.3	(48)
AVR2	N-terminal GFP	0.2	(66)
Rpi-blb1	Untagged	0.6	(51, 67)
AVRblb1	N-terminal GFP	0.6	(67)
R3a	Untagged	0.3	(19)
AVR3a^{KI}	Untagged	0.2	(19)
BS4	C-terminal Myc	0.4	(68)
AvrBs3	Untagged	0.4	(68)

References.

1. Wu CH, Belhaj K, Bozkurt TO, Birk MS, & Kamoun S (2016) Helper NLR proteins NRC2a/b and NRC3 but not NRC1 are required for Pto-mediated cell death and resistance in Nicotiana benthamiana. *New Phytol* 209(4):1344-1352.
2. Weber E, Engler C, Gruetzner R, Werner S, & Marillonnet S (2011) A modular cloning system for standardized assembly of multigene constructs. *Plos One* 6(2):e16765.
3. Engler C*, et al.* (2014) A golden gate modular cloning toolbox for plants. *ACS Synth Biol* 3(11):839-843.
4. Liu Y, Schiff M, & Dinesh-Kumar SP (2002) Virus-induced gene silencing in tomato. *Plant J* 31(6):777-786.
5. Peart JR*, et al.* (2002) Ubiquitin ligase-associated protein SGT1 is required for host and nonhost disease resistance in plants. *Proc Natl Acad Sci U S A* 99(16):10865-10869.
6. Song J*, et al.* (2009) Apoplastic effectors secreted by two unrelated eukaryotic plant pathogens target the tomato defense protease Rcr3. *Proc Natl Acad Sci U S A* 106(5):1654-1659.
7. Zhu S, Li Y, Vossen JH, Visser RG, & Jacobsen E (2012) Functional stacking of three resistance genes against *Phytophthora infestans* in potato. *Transgenic Res* 21(1):89-99.
8. Giannakopoulou A*, et al.* (2015) Tomato I2 immune receptor can be engineered to confer partial resistance to the oomycete *Phytophthora infestans* in addition to the fungus *Fusarium oxysporum*. *Mol Plant Microbe Interact* 28(12):1316-1329.
9. Tameling WIL & Baulcombe DC (2007) Physical association of the NB-LRR resistance protein Rx with a Ran GTPase-activating protein is required for extreme resistance to Potato virus X. *Plant Cell* 19(5):1682-1694.
10. Kim SH, Qi D, Ashfield T, Helm M, & Innes RW (2016) Using decoys to expand the recognition specificity of a plant disease resistance protein. *Science* 351(6274):684-687.
11. Du J, Rietman H, & Vleeshouwers VG (2014) Agroinfiltration and PVX agroinfection in potato and *Nicotiana benthamiana*. *J Vis Exp* (83):e50971.
12. Petre B*, et al.* (2016) Heterologous expression screens in *Nicotiana benthamiana* identify a candidate effector of the wheat yellow rust pathogen that associates with processing bodies. *Plos One* 11(2):e0149035.
13. Balmuth A & Rathjen JP (2007) Genetic and molecular requirements for function of the Pto/Prf effector recognition complex in tomato and Nicotiana benthamiana. *Plant J* 51(6):978-990.
14. Wei CF*, et al.* (2007) A *Pseudomonas syringae* pv. *tomato* DC3000 mutant lacking the type III effector HopQ1-1 is able to cause disease in the model plant *Nicotiana benthamiana*. *Plant J* 51(1):32-46.
15. Brommonschenkel SH, Frary A, Frary A, & Tanksley SD (2000) The broad-spectrum tospovirus resistance gene Sw-5 of tomato is a homolog of the root-knot nematode resistance gene Mi. *Mol Plant Microbe Interact* 13(10):1130-1138.
16. Spassova MI*, et al.* (2001) The tomato gene *Sw5* is a member of the coiled coil, nucleotide binding, leucine-rich repeat class of plant resistance genes and confers resistance to TSWV in tobacco. *Molecular Breeding* 7(2):151-161.
17. Hallwass M*, et al.* (2014) The *Tomato spotted wilt virus* cell-to-cell movement protein (NSm) triggers a hypersensitive response in *Sw-5*-containing resistant tomato lines and in *Nicotiana benthamiana* transformed with the functional *Sw-5b* resistance gene copy. *Mol Plant Pathol* 15(9):871-880.

18. Peiro A, *et al.* (2014) The movement protein (NSm) of *Tomato spotted wilt virus* is the avirulence determinant in the tomato *Sw-5* gene-based resistance. *Mol Plant Pathol* 15(8):802-813.

19. Bos JI, *et al.* (2006) The C-terminal half of *Phytophthora infestans* RXLR effector AVR3a is sufficient to trigger R3a-mediated hypersensitivity and suppress INF1-induced cell death in *Nicotiana benthamiana*. *Plant J* 48(2):165-176.

20. Segretin ME, *et al.* (2014) Single amino acid mutations in the potato immune receptor R3a expand response to *Phytophthora* effectors. *Mol Plant Microbe Interact* 27(7):624-637.

21. Andolfo G, *et al.* (2014) Defining the full tomato NB-LRR resistance gene repertoire using genomic and cDNA RenSeq. *BMC Plant Biol* 14:120.

22. Kumar S, Stecher G, & Tamura K (2016) MEGA7: molecular evolutionary genetics analysis version 7.0 for bigger datasets. *Mol Biol Evol* 33(7):1870-1874.

23. Steuernagel B, Jupe F, Witek K, Jones JD, & Wulff BB (2015) NLR-parser: rapid annotation of plant NLR complements. *Bioinformatics* 31(10):1665-1667.

24. Katoh K & Standley DM (2013) MAFFT multiple sequence alignment software version 7: improvements in performance and usability. *Mol Biol Evol* 30(4):772-780.

25. Huang S, *et al.* (2013) Draft genome of the kiwifruit *Actinidia chinensis*. *Nat Commun* 4:2640.

26. Denoeud F, *et al.* (2014) The coffee genome provides insight into the convergent evolution of caffeine biosynthesis. *Science* 345(6201):1181-1184.

27. Harper AL, *et al.* (2016) Molecular markers for tolerance of european ash (*Fraxinus excelsior*) to dieback disease identified using associative transcriptomics. *Sci Rep* 6:19335.

28. Dohm JC, *et al.* (2014) The genome of the recently domesticated crop plant sugar beet (*Beta vulgaris*). *Nature* 505(7484):546-549.

29. Azevedo C, *et al.* (2006) Role of SGT1 in resistance protein accumulation in plant immunity. *EMBO J* 25(9):2007-2016.

30. van der Vossen EAG, *et al.* (2005) The Rpi-blb2 gene from Solanum bulbocastanum is an Mi-1 gene homolog conferring broad-spectrum late blight resistance in potato. *Plant J* 44(2):208-222.

31. Milligan SB, *et al.* (1998) The root knot nematode resistance gene Mi from tomato is a member of the leucine zipper, nucleotide binding, leucine-rich repeat family of plant genes. *Plant Cell* 10(8):1307-1319.

32. Tran PT, Choi H, Choi D, & Kim KH (2015) Molecular characterization of Pvr9 that confers a hypersensitive response to Pepper mottle virus (a potyvirus) in Nicotiana benthamiana. *Virology* 481:113-123.

33. Ernst K, *et al.* (2002) The broad-spectrum potato cyst nematode resistance gene (*Hero*) from tomato is the only member of a large gene family of NBS-LRR genes with an unusual amino acid repeat in the LRR region. *Plant J* 31(2):127-136.

34. Vossen JH, *et al.* (2016) The Solanum demissum R8 late blight resistance gene is an Sw-5 homologue that has been deployed worldwide in late blight resistant varieties. *Theor Appl Genet* 129(9):1785-1796.

35. Ballvora A, *et al.* (2002) The R1 gene for potato resistance to late blight (Phytophthora infestans) belongs to the leucine zipper/NBS/LRR class of plant resistance genes. *Plant J* 30(3):361-371.

36. Salmeron JM, *et al.* (1996) Tomato *Prf* is a member of the leucine-rich repeat class of plant disease resistance genes and lies embedded within the *Pto* kinase gene cluster. *Cell* 86(1):123-133.

37. Bendahmane A, Kanyuka K, & Baulcombe DC (1999) The Rx gene from potato controls separate virus resistance and cell death responses. *Plant Cell* 11(5):781-791.

38. Bendahmane A, Querci M, Kanyuka K, & Baulcombe DC (2000) Agrobacterium transient expression system as a tool for the isolation of disease resistance genes: application to the *Rx2* locus in potato. *Plant J* 21(1):73-81.

39. van der Vossen EA, *et al.* (2000) Homologues of a single resistance-gene cluster in potato confer resistance to distinct pathogens: a virus and a nematode. *Plant J* 23(5):567-576.

40. Tai TH, *et al.* (1999) Expression of the Bs2 pepper gene confers resistance to bacterial spot disease in tomato. *P Natl Acad Sci USA* 96(24):14153-14158.

41. Witek K, *et al.* (2016) Accelerated cloning of a potato late blight-resistance gene using RenSeq and SMRT sequencing. *Nat Biotechnol* 34(6):656-660.

42. Foster SJ, *et al.* (2009) *Rpi-vnt1.1*, a *Tm-2(2)* homolog from *Solanum venturii*, confers resistance to potato late blight. *Mol Plant Microbe Interact* 22(5):589-600.

43. Pel MA, *et al.* (2009) Mapping and cloning of late blight resistance genes from *Solanum venturii* using an interspecific candidate gene approach. *Mol Plant Microbe Interact* 22(5):601-615.

44. Lanfermeijer FC, Dijkhuis J, Sturre MJ, de Haan P, & Hille J (2003) Cloning and characterization of the durable tomato mosaic virus resistance gene *Tm-2(2)* from *Lycopersicon esculentum*. *Plant Mol Biol* 52(5):1037-1049.

45. Smilde WD, Brigneti G, Jagger L, Perkins S, & Jones JD (2005) *Solanum mochiquense* chromosome IX carries a novel late blight resistance gene *Rpi-moc1*. *Theor Appl Genet* 110(2):252-258.

46. Jo KR, Visser RG, Jacobsen E, & Vossen JH (2015) Characterisation of the late blight resistance in potato differential *MaR9* reveals a qualitative resistance gene, *R9a*, residing in a cluster of *Tm-2 (2)* homologs on chromosome IX. *Theor Appl Genet* 128(5):931-941.

47. Zhang C, *et al.* (2013) Fine mapping of the *Ph-3* gene conferring resistance to late blight (*Phytophthora infestans*) in tomato. *Theor Appl Genet* 126(10):2643-2653.

48. Lokossou AA, *et al.* (2009) Exploiting knowledge of R/Avr genes to rapidly clone a new LZ-NBS-LRR family of late blight resistance genes from potato linkage group IV. *Mol Plant Microbe Interact* 22(6):630-641.

49. Park TH, *et al.* (2005) The late blight resistance locus *Rpi-blb3* from *Solanum bulbocastanum* belongs to a major late blight R gene cluster on chromosome 4 of potato. *Mol Plant Microbe In* 18(7):722-729.

50. Haverkort AJ, *et al.* (2016) Durable late blight resistance in potato through dynamic varieties obtained by cisgenesis: scientific and societal advances in the DuRPh project. *Potato Res* 59(1):35-66.

51. van der Vossen E, *et al.* (2003) An ancient R gene from the wild potato species *Solanum bulbocastanum* confers broad-spectrum resistance to *Phytophthora infestans* in cultivated potato and tomato. *Plant J* 36(6):867-882.

52. Ori N, *et al.* (1997) The I2C family from the wilt disease resistance locus I2 belongs to the nucleotide binding, leucine-rich repeat superfamily of plant resistance genes. *Plant Cell* 9(4):521-532.

53. Huang S, *et al.* (2005) Comparative genomics enabled the isolation of the *R3a* late blight resistance gene in potato. *Plant J* 42(2):251-261.

54. Li G, *et al.* (2011) Cloning and characterization of *R3b;* members of the *R3* superfamily of late blight resistance genes show sequence and functional divergence. *Mol Plant Microbe Interact* 24(10):1132-1142.

55. Tomita R, *et al.* (2011) Genetic basis for the hierarchical interaction between *Tobamovirus* spp. and L resistance gene alleles from different pepper species. *Mol Plant Microbe In* 24(1):108-117.

56. Bozkurt TO, *et al.* (2011) *Phytophthora infestans* effector AVRblb2 prevents secretion of a plant immune protease at the haustorial interface. *Proc Natl Acad Sci U S A* 108(51):20832-20837.

57. Lu R, *et al.* (2003) High throughput virus-induced gene silencing implicates heat shock protein 90 in plant disease resistance. *EMBO J* 22(21):5690-5699.

58. Schornack S, *et al.* (2010) Ancient class of translocated oomycete effectors targets the host nucleus. *Proc Natl Acad Sci U S A* 107(40):17421-17426.

59. Oh SK, *et al.* (2009) In Planta Expression Screens of Phytophthora infestans RXLR Effectors Reveal Diverse Phenotypes, Including Activation of the Solanum bulbocastanum Disease Resistance Protein Rpi-blb2. *Plant Cell* 21(9):2928-2947.

60. Segonzac C, *et al.* (2011) Hierarchy and roles of pathogen-associated molecular pattern-induced responses in *Nicotiana benthamiana*. *Plant Physiol* 156(2):687-699.

61. Lukasik-Shreepaathy E, *et al.* (2012) Dual regulatory roles of the extended N terminus for activation of the tomato MI-1.2 resistance protein. *Mol Plant Microbe Interact* 25(8):1045-1057.

62. Du Y, Berg J, Govers F, & Bouwmeester K (2015) Immune activation mediated by the late blight resistance protein R1 requires nuclear localization of R1 and the effector AVR1. *New Phytol* 207(3):735-747.

63. de Vries JS, Andriotis VM, Wu AJ, & Rathjen JP (2006) Tomato *Pto* encodes a functional N-myristoylation motif that is required for signal transduction in *Nicotiana benthamiana*. *Plant J* 45(1):31-45.

64. Rathjen JP, Chang JH, Staskawicz BJ, & Michelmore RW (1999) Constitutively active Pto induces a Prf-dependent hypersensitive response in the absence of avrPto. *EMBO J* 18(12):3232-3240.

65. Pel MA (2010) Mapping, isolation and characterization of genes responsible for late blight resistance in potato. *Ph.D. Thesis. Wageningen University, the Netherlands*.

66. Saunders DG, *et al.* (2012) Host protein BSL1 associates with *Phytophthora infestans* RXLR effector AVR2 and the *Solanum demissum* immune receptor R2 to mediate disease resistance. *Plant Cell* 24(8):3420-3434.

67. Vleeshouwers VG, *et al.* (2008) Effector genomics accelerates discovery and functional profiling of potato disease resistance and *Phytophthora infestans* avirulence genes. *Plos One* 3(8):e2875.

68. Schornack S, *et al.* (2004) The tomato resistance protein Bs4 is a predicted non-nuclear TIR-NB-LRR protein that mediates defense responses to severely truncated derivatives of AvrBs4 and overexpressed AvrBs3. *Plant J* 37(1):46-60.